EFFECTS OF SPATIAL VARIABILITY OF RAINFALL ON RUNOFF AND SOIL EROSION: A CASE STUDY IN RIBEIRA SECA CATCHMENT, SANTIAGO ISLAND, CAPE VERDE

HAILEMARIAM KEBEDE BILISA
April, 2013

SUPERVISORS:
Dr. ir. J. (Janneke) Ettema
Dr. D.B. (Dhruba) Pikha Shrestha

EFFECTS OF SPATIAL VARIABILITY OF RAINFALL ON RUNOFF AND SOIL EROSION: A CASE STUDY IN RIBEIRA SECA CATCHMENT, SANTIAGO ISLAND, CAPE VERDE
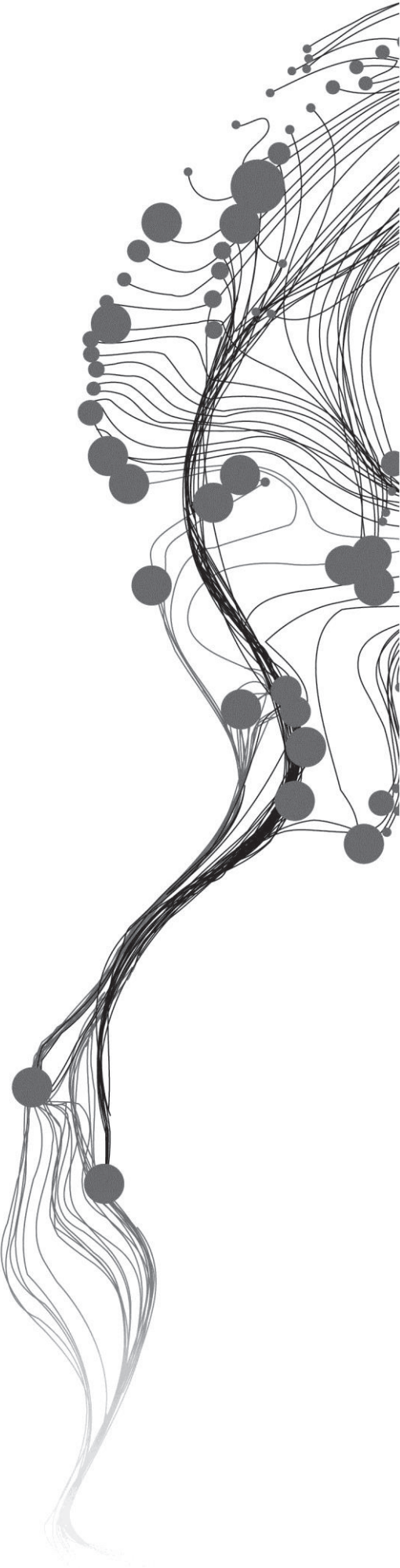
HAILEMARIAM KEBEDE BILISA

Enschede, The Netherlands, April, 2013

Thesis submitted to the Faculty of Geo-Information Science and Earth Observation of the University of Twente in partial fulfilment of the requirements for the degree of Master of Science in Geo-information Science and Earth Observation.
Specialization: Environmental and Engineering Geology

SUPERVISORS:
Dr. ir. J. (Janneke) Ettema
Dr. D.B. (Dhruba) Pikha Shrestha

THESIS ASSESSMENT BOARD:
Prof. dr. V.G. (Victor) Jetten (Chair)
Dr. ir. C.M.M. (Chris) Mannaerts (External Examiner, ITC, University of Twente)

Dedicated to:

My mom: **Gete Gebeyehu Hoda** (before 1990 G.C)
'Geexee Gabayoo Hodaa'

&

My beloved sister: **Birke Kebede Bilisa**

ABSTRACT

Soil erosion is a land surface degradation process caused by water and wind, and aggravated by human activities. Runoff is one of the main causes of soil erosion. The impact of soil erosion is more serious in developing countries and in arid to semi-arid environments around the world. Many studies have been conducted to model runoff and soil erosion in particular study areas around the world to understand the diverse effects of soil erosion and runoff on economic and social activities. Policy makers and planning agencies at various levels need quantitative evaluation of the extent and magnitude of soil erosion and runoff problems to develop conservation measures to guard the landscape and prevent soil erosion.

Rainfall-runoff modeling helps in providing the opportunity to understand the hydrological response of a watershed. Rainfall measured either by rain gauges or estimated by satellite is the main inputs of runoff and soil erosion modeling. Event based models are able to evaluate the effect of single events on runoff and soil erosion. Limburg Soil erosion Model (LISEM), a newly developed hydrological and soil erosion model is one of the main physically based event model. Rainfall from satellite, which takes in to account the spatial variability of rainfall hasn't been yet used as an input to LISEM model to simulate runoff and soil erosion processes.

This study is conducted in medium sized (71.5 km²) Ribeira Seca catchment, Santiago Island, Cape Verde. The main objectives of the study are: (i) to compare the Meteosat Second Generation Multi-sensor Precipitation Estimate (MSGMPE) estimated rainfall to ground (rain gauge and disdrometer) measured rainfall and (ii) to examine the effects of spatial variability of rainfall on runoff and soil erosion.

The results obtained from the 15 minutes based temporal resolution comparisons of the rainfall depth estimated by MSGMPE and measured by disdrometer at a single location in the catchment reveal poor correlation. A maximum correlation with coefficient of determination R^2 equals 0.35 is obtained. However, correlation is improved as the 15 minutes rainfalls are aggregated to daily rain depth and compared. Daily based monthly and yearly comparisons of rain depth from MSGMPE to ground measurements resulted in up to R^2 equals 0.9 and 0.6, respectively. 2009 was the year with poor correlation; whereas, 2010 was the year with the best correlation obtained between ground and satellite based rainfall measurements.

OpenLISEM v1.56 is applied to Ribeira Seca catchment with homogeneous and spatially variable rainfall to simulate runoff and soil erosion. Since, the total rainfall that is derived from the MSGMPE over the entire catchment was lower that derived from disdrometer for the selected rainfall event, a ratio correction factor was used. Despite the same amount of rainfall over the entire catchment from both sources, the total discharge and erosion results were different. However, the spatial patterns of infiltration, runoff and erosion from both rainfall inputs were found to be similar and appear to follow the soil properties. The discharge to rainfall ratio from MPE rainfall input was 41%; whereas, that from homogeneous rainfall input was 26 %. This is attributed to either the low intensity or spatial variability of rainfall from MSGMPE, which makes the water to infiltrate as compared to the disdrometer rainfall. The sediment delivery ratio obtained from the homogenous rainfall input at the main outlet of the catchment (17.1 %) was about three-fold higher than the spatially variable MSGMPE derived rainfall input, which is 6.02 %.

 Key words: Ribeira Seca, LISEM, MSGMPE, disdrometer, rainfall events, runoff, soil erosion.

ACKNOWLEDGEMENTS

TABLE OF CONTENTS

LIST OF FIGURES

LIST OF TABLES

LIST OF APPENDICES

NOMENCLATURE

ALOS-AVNIR	Advanced Land Observation Satellite-Advanced Visible and Near Infrared Radiometer
DEM	Digital Elevation Model
ESA	European Space Agency
EUMETSAT	EUropean organization for the exploitation of METeorological SATellite
EVI	EVent Index
GMS	Geostationary Meteorological Satellite
GOES	Geostationary Operational Environmental Satellite
ILWIS	Integrated Land and Water Information System (software)
ITC	Faculty of Geo-information Science and Earth observation, The Netherlands
K_s	Saturated Hydraulic Conductivity
LDD	Local Drain Direction
LISEM	Limburg Soil Erosion Model
mm	Millimeter
mm h^{-1}	Millimeter per hour
MSG	Meteosat Second Generation
MSGMPE	Meteosat Second Generation Multi-sensor Precipitation Estimate
n	Manning's/Random roughness
NOAA	National Oceanic and Atmospheric Administration
RUSLE	Revised Universal Soil Loss Equation
SDR	Sediment Delivery Ratio
SRTM	Shuttle Radar Topography Mission
TRMM	Tropical Rainfall Measuring Mission
USLE	Universal Soil Loss Equation
UTM	Universal Transverse Mercator
EUROSEM	EUROpean Soil Erosion Model

1. INTRODUCTION

1.1   Research backgroud

Soil erosion is a long term and almost imperceptible land surface degradation process that can be caused by water or wind. Its aggravation by human activities has been one of the major problems affecting the livelihoods of humans around the world. Accelerated soil erosion is a widespread problem for the fact that it has an influence on environmental quality, agricultural productivity, food security, among others in many countries of the world (Lal, 2001; R.P.C. Morgan, 2005; Pimentel et al., 1995). The impact of soil erosion on economy and society is more serious in developing countries than those which are developed. In developing countries, the livelihood of a large majority of the populations is directly dependent on agriculture and other land resources.

Even though soil erosion is known to be the major economic and environmental problem around the world, its extent, severity, and economic and environmental impacts are diverse (Lal, 2001). Policy makers and planning agencies at various levels frequently need a quantitative evaluation of the extent and magnitude of the soil erosion problems to develop the possible management strategies on a local, regional and global basis. Since the impacts of soil erosion is both on-site and off-site, the management plans need to consider both problems. The on-site impacts refers to the loss of soil from field, the break-down of soil structure, and the decline of organic matter and nutrients, leading to a decline in soil fertility and in the end to a reduced food security and vegetation cover (Stocking, 2003). The off-site effects of erosion include sedimentation problems in river channels, increased flood risk and reduced life time of reservoirs in the downstream areas, siltation of agricultural areas, water logging among others (Haregeweyn et al., 2006; Verstraeten & Poesen, 1999).

In dry and semi-arid areas such as sub-Saharan countries, weather affects rainfall patterns. In semi-arid regions, characterized by low annual rainfall but with occurrence of high intensities, variation in precipitation patterns may affect local runoff, soil erosion and sediment yield (Sánchez-Moreno et al., 2008). For example, study (Mannaerts & Gabriels, 2000), in Cape Verde (one of the semi-arid environment country), reveal that even though the amount of monthly and annual rainfall is low, the variation of daily or storm precipitation are very high. Due to this reason, it is vital to know the location and amount of rain entering in to the basin system and consider storms for realistic prediction of runoff, sediments yield and erosion occurring in the catchments (Ran et al., 2012; Sánchez-Moreno et al., 2008).

Although high-intensity rainfall events are often held responsible for the main part of soil erosion in semi-arid areas (Baartman et al., 2012), accurate spatial and temporal rainfall estimates are still lacking. In most of the developing countries, rain gauges are either lacking or sparsely distributed in a particular watershed. Interpolating rainfall products from sparsely distributed rain gauges over a range of an area makes rough estimation of rainfall. Therefore, for spatial characterization of rainfall, remote sensing techniques rainfall acquisition are appropriate for areas with sparse rain gauge distributions (Sánchez-Moreno et al., 2008).

The type and magnitude of erosion processes determines the selection of appropriate conservation practices (Capra et al., 2005) for mitigation of soil erosion. In order to reduce both on-site and off-site impacts of soil erosion, different types of conservation measures are usually practiced in areas prone to soil erosion. For example, In Cape Verde, slanting terraces, planting vegetation, construction of small check dams across the small streams are among the conservation practices used (DESIRE, 2012). This mitigation measures aims at providing certain degree of permanent soil cover to serve as shield for the impact of rain. Despite these efforts, the risk of soil erosion and degradation is very high in most cases (DESIRE, 2012).

In order to install conservation measures so as to guard the landscape and prevent soil erosion, it is important to know which locations in a watershed are frequently degraded. It is apparent that erosion is caused by runoff, which in turn depends on relief, rainfall and soil properties. Previous studies of soil erosion models as for example by

Universal Soil Loss Equation (USLE) only takes in to account soil and relief properties. Therefore, the conservation measure to be taken that could be advised based on the results from these models only depends on these two properties.

However, runoff and soil erosion modelling should take in to account the hydrological process and the flow direction in a given watershed. Hence, for assessment of runoff and soil erosion process in the area, a physically based event model is chosen in this study. Event-based models are suited for the purpose of evaluating single events. Other landscape models which use average annual rainfall as an input are unable to evaluate single events (Coulthard et al., 2002) . This study presents the effect of the spatial and temporal variation of rainfall, derived from satellite sensors on runoff and soil erosion processes. Due to its high temporal and spatial resolution as compared to other satellite precipitation estimates, the Meteosat Second Generation precipitation Estimate (MSGMPE) was chosen for this study.

This study is particularly conducted in Ribeira Seca catchment, Santiago Island with the main focus on the assessing runoff and soil erosion over the entire catchment. Since Ribeira Seca catchment is the main agricultural area and with very sparse vegetation, it is susceptible to runoff and soil erosion. The catchment receives short duration of rainfall with high intensity every year. Runoff and soil erosion modeling assessments conducted in the catchment so far have not been yet taking into account the spatial variability of rainfall. Therefore, the Limburg Soil Erosion Model (LISEM) was applied to Ribeira Seca catchment with homogeneous and spatially variable rainfall as an input to assess runoff and soil erosion.

1.2   Problem statement

Rainfall characteristics (Assouline et al., 2007; C. L. Chang, 2007; Ran et al., 2012) and watershed characteristics (Assouline & Mualem, 2006; Broxton et al., 2009) are the two primary factors affecting runoff generation and soil erosion. Rainfall is one of the main inputs for runoff and soil erosion modeling. However, rainfall is the most difficult to measure among the hydrological parameters due to its temporal and spatial variation, and discontinuity nature (Jeniffer et al., 2010). The prediction of runoff and soil erosion by models, which uses rainfall as input are mostly good in areas where the rain gauges are densely distributed. However, quantitative simulation models of surface runoff and soil erosion, which can be used to evaluate alternative strategies for improved land management, not only in the monitored areas but also in ungauged catchments, are useful.

Previous studies (Baartman et al., 2012; Kværnø & Stolte, 2012) used rainfall inputs that are generated from measurements of the sparsely distributed rain-gauges as an input for LISEM model. These rainfall inputs were obtained from interpolating the available rain gauge measurements. However, in most cases, in areas with sparse rain gauges distributions, this interpolation doesn't provide very good information on the spatial variation of rainfall for the locations between rain gauges. Nevertheless, rainfall in most cases is virtually variable over a given area of interest particularly in semi-arid regions. Hence, the use of satellite rainfall estimates as an alternative for such areas with either no rain gauges or where rain gauges are sparsely distributed in a given watershed is crucial. Furthermore, satellite rainfall estimates takes in to account the spatial variability of rainfall over an area under study.

Most modeling studies conducted to simulate runoff and soil erosion so far did not yet take into account the spatial variability of rainfall over a region under study. On one hand, the reason could be due to unavailability of the model having the ability to simulate spatial patterns of erosion. On the other hand, the main problem is getting rainfall data representing all the spatial and temporal variation. In many cases, data from only few rain gauges are available which could be attributed to either the sparseness of the gauge network, or the available gauges are not automatic. In some cases, we have to assume that rainfall is homogeneous simply because of unavailability of sufficient meteorological stations. Furthermore, the usability of satellite derived rainfall estimates varies due to the different input requirements of the type of runoff and soil erosion models employed. In addition, the rainfall products from satellites come at different spatial and temporal resolutions, making their usability different.

In semi-arid environments, heavy rainfall events could generate runoff and soil erosion by two mechanisms called Hortonian overland flow and saturated overland flow (Sanchez Moreno et al., 2012b). Cape Verde archipelago is one of the countries located in semi-arid environments. High erosion rates occur during heavy rainfall events is considered the most critical environmental and agricultural problem in Cape Verde. Ribeira Seca catchment, which is the subject of this study, is the biggest watershed in Santiago Island. The low soil cover and, rugged relief and inadequate practice of rain-fed agriculture in the catchment made it susceptible to runoff and soil erosion (DESIRE, 2012). At the beginning of the rainy season when the soil has little or no vegetation cover, extreme rainfall events are the main cause of runoff and soil erosion in Ribeira Seca catchment, particularly in steep slopes (Sanchez Moreno et al., 2012b). This suggests a model which considers rainfall events has to be used for estimation of runoff and soil erosion. Only one rain gauge is found in Ribeira Seca catchment (71.5 km²). Therefore, satellite rainfall estimates are the best alternative (also cost effective) for such area to estimate the precipitation over the whole entire catchment. Hence, LISEM, an event based model, is applied to simulate runoff and soil erosion processes in Ribeira Seca catchment with spatially variable and homogeneous rainfall.

1.3   Research objectives, questions and hypotheses

The general objective of this research is to characterize the effect of rainfall spatial variability on runoff and soil erosion in medium-sized Ribeira Seca catchment, Santiago Island, Cape Verde.

1.3.1   Specific objectives

The sub-objectives of the research to attain the main objective are:-

a) To compare the rainfall estimates from Meteosat Second Generation Multi-sensor Precipitation Estimate (MSGMPE) with ground based rainfall measurements.

b) To examine the effect of different correction and interpolation techniques of MSGMPE rainfall as an input to the runoff and soil erosion model applied to a medium-sized catchment.

c) To characterize the effect of the spatial variability of rainfall on the simulated infiltration, runoff and soil erosion processes in the catchment, compared to a spatially homogeneous rainfall.

1.3.2   Research questions

a) How does satellite-derived rainfall correlate to the rain gauge and disdrometer measurements?

b) Which interpolation (down scaling 3 km MSGMPE to 20 m) method would give better simulation of runoff and soil erosion?

c) What are the temporal and spatial patterns of runoff and erosion processes within the watershed in homogeneous and spatially variable rainfall?

d) What is the difference in soil loss from the watershed in homogeneous rainfall and spatially variable rainfall?

1.3.3   Hypothesis

a) Rainfall spatial variability is one of the main factors affecting the runoff and sediment leaving the watershed.

b) There is a difference in runoff and soil erosion pattern simulated by the model in the watershed from spatially variable and homogeneous rainfall inputs.

1.4   Thesis structure

The overall structure of the thesis is illustrated in Figure 1-1; and the brief descriptions of each chapters are summarized below.

CHAPTER 1: includes the background, problem statement, objectives, questions and hypothesis about this research.

CHAPTER 2: shows the literature review in brief about rainfall from ground measurements and satellite estimates, and runoff and erosion modeling.

CHAPTER 3: explains in detail the materials used and the methods followed to compare the rainfall from ground measurement with satellite estimate, and prepare the rainfall input for LISEM model.

CHAPTER 4: describes the rainfall comparison results and discussions, and the selection of event.

CHAPTER 5: describes runoff and soil erosion related modeling.

CHAPTER 6: includes summary, attempts to answer the research questions, conclusions and recommendations.
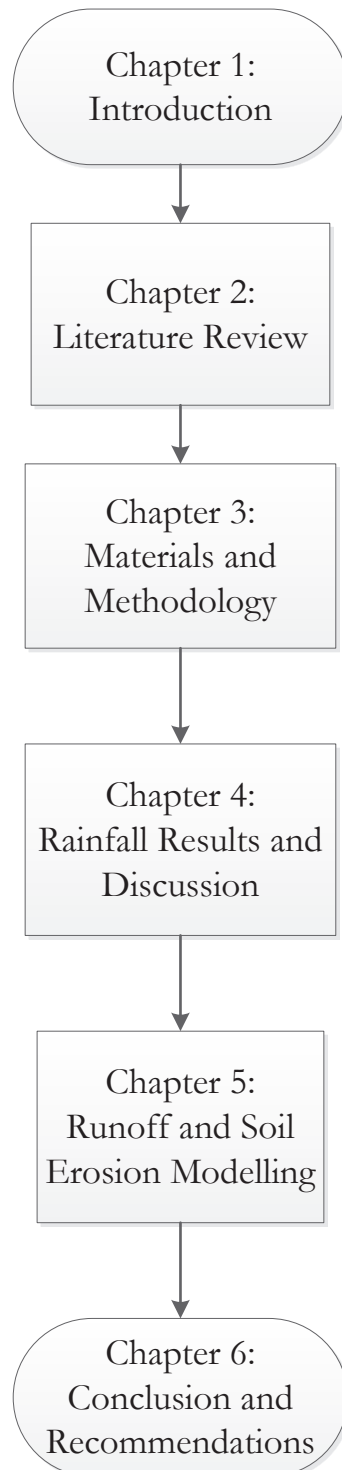
Figure 1-1: Outline of the thesis.

2.   LITERATURE REVIEW

2.1   Introduction

Erosion and deposition are among the main processes that shape the landscape over time. Runoff is one of the main causes of erosion and deposition of the eroded soil material. Erosion is the general term that refers to all eroding process occurring in a watershed or drainage basin, whereas soil erosion is limited to erosion (approximately the upper meter from the soil surface) process of soil material (de Vente et al., 2008). To assess the runoff, sediment detachment and sediment leaving a given watershed by modeling, a number of input parameters are required which in turn depends on the type of soil erosion models employed.

Diverse soil erosion models have been developed that can be grouped in to three main classes (Merritt et al., 2003). These are empirical or statistical/metric models, conceptual models and physically based models. Physically-based models use equations of conservation of mass and momentum for both sediment and flow simulations, and usually require a large amount of measurement data. OpenLISEM (Baartman et al., 2012; De Roo et al., 1996a) is an example of physically-based model that require high temporal resolution of rainfall data for single events.

For realistic estimation of runoff, sediment delivery ratio and soil erosion by modeling, it is important to know the amount of water that enters into a watershed. The average soil loss in the watershed per rain event increases with increasing the intensity of the rain storm (R.P.C. Morgan & Davidson, 1986). Although there could be a variation from one storm to another, erosion is almost entirely caused by rainfall intensities higher than 25 mm h^{-1} (Hudson, 1986; R.P.C. Morgan & Davidson, 1986). Morgan et al., (1986) added that the role of intensity is not always clear, but it appears that erosion is related to two types of rain event. These are the short-lived intense storms in which the infiltration capacity of the soil is exceeded, and the prolonged low intensity storm which saturates the soil; therefore, resulting in soil erosion. Hessel et al., (2003b) pointed out the importance of relating rainfall event with the discharge data. A high intensity rainfall does not always necessarily translate in to a large amount of discharge in a given watershed due to the soil moisture condition, land use type, among many others. In areas with lack of dense rain gauges and/or where rainfall is measured at coarse time interval, satellite derived precipitation becomes the only source as an input for erosion models. Nevertheless, there is no a single spaceborne platform which carries all the suitable instruments for monitoring the properties related to rainfall occurrence. Therefore, the problem of using satellite remote sensing to retrieve rainfall at a desired spatial and temporal resolutions for a specific area remains complicated (Maathuis et al., 2006).

The following sub-sections describe the summary of previous studies. In the first case, rainfall measurements (ground and satellite) will be described followed by runoff and erosion modelling, and LISEM model descriptions.

2.2   Rainfall measurements

2.2.1   Rainfall from gauges

For an integrated watershed management, the quantification of individual components of the hydrologic cycle at the catchment scale is a crucial step (Jeniffer et al., 2010). Rainfall is one of the main inputs for simulation of the response of a given watershed to runoff and erosion processes. Jeniffer et al., (2010) added, the predictions from rainfall-runoff models are often unsatisfactory due to the temporal and spatial variability of rainfall over a region of interest. Traditionally, rainfall is measured by conventional rain gauges. Measurements of rainfall by conventional rain gauges provide relatively accurate estimates of rain. But their accuracy is limited at a few points of a region around the location of the rain gauges (Collischonn et al., 2008; Haile et al., 2010; Jeniffer et al., 2010; Prasetia et al., 2012; Prigent, 2010). In many hydrological related studies, the rain field for the rest of the region under interest is estimated by interpolating the available rain gauge data. Nevertheless, this interpolation provides very rough estimates of the actual rain fields in locations where the rain gauges are sparsely distributed. This is particularly true

for tropical regions where most rainfall has a convective origin with high spatial variability at the daily level (Collischonn et al., 2008), and is typical in most of the developing countries like Cape Verde. Only one rain gauge is found in the Ribeira Seca catchment from station San Jorge.

2.2.2   Rainfall from satellite

Estimation of rainfall by remote sensing is very useful in regions such as Cape Verde, where rain gauge density is very low and rainfall highly variable. Several satellites which use diverse sensors for global or regional precipitation measurements are available. Some of the most known satellite missions are: TRMM, NOAA, GOES, GMS, MSG among others (Kidd & Huffman, 2011; Tapiador et al., 2012) and new missions are under development (Thies & Bendix, 2011). Diverse precipitation products from these satellites are available which are obtained from various algorithms that transform radiances emitted or scattered from clouds or raindrops into precipitation (Amato et al., 2008; Ebert & Manton, 1998; Salvador et al., 2013). There are several methods to estimate rain rates from satellite images, from several bands of the electromagnetic spectrum (Collischonn et al., 2008). The estimation is useful if a high spatial resolution, rapid revisiting time and adequate accuracy could be achieved (Prigent, 2010). However, the precision of these estimates depends on the algorithms employed and the ground data used for calibration.

Precipitation estimates from satellites are based upon observations in the visible/infrared or in the microwave. Measurements in the visible (VIS) and infrared (IR) spectrum provide information only on the top of the cloud that generates rain; therefore, the precipitation estimate is thus indirect (Collischonn et al., 2008; Maathuis et al., 2006; Prigent, 2010). Despite this limitation, the products from those satellites have better spatial and temporal resolution, making them vital for the prediction of spatial and temporal variation of rainfall as an input in physically based models like LISEM. Due to their geostationary position at Longitude 00 (respectively 6.5 west for Meteosat-8 at present) above the equator (Latitude 00), Meteosat Second Generation (MSG) satellites are relevant for Europe and Africa (Sánchez-Moreno et al., 2008). MSG is a new generation of geostationary satellites developed by European Space Agency (ESA) and European organization for the exploitation of METeorological SATellite (EUMETSAT). It is one of the geostationary satellites in the equatorial plane at an altitude of about 36,000km above the earth having the same revolution time as the earth itself and therefore always viewing the same area. The Spinning Enhanced Visible and Infrared Instrument (SEVIRI) on board the MSG provides a potential for better characterization of clouds by means of improved infrared calibration, radiometric performances, multi-spectral information (12 channels), high spatial (3km at sub-satellite point) and temporal resolution (15 minute for the full disk) (Jeniffer et al., 2010; Prigent, 2010). Jeniffer et al., (2010) added the High Resolution Visible (HRV) channel of MSG has a sampling distance interval of about 1km besides the 3km at nadir. Moreover, the repeat cycle of 15 minute full disk imaging provides multi-spectral observations of rapidly changing deep convection.

2.3   Runoff and soil erosion modeling

To characterize runoff and soil erosion process in catchments, a model which takes in to account, physical processes has to be applied. The catchment or drainage basin is often chosen as the system to be modelled since it can be delineated easily under most natural conditions. There are wide ranges of runoff and soil erosion models exist. However, the application of these models depends on the purpose (objective of the study), scale and resolution of the model and the available data to be used as input to the model. Models exist for all scales ranging from small plots to continental (Jetten & Favis-Mortlock, 2006).

The diverse soil erosion models developed so far can be grouped in to three main classes (Merritt et al., 2003). These are empirical models, conceptual models and physically based models. In general, empirical or statistical/metric models are simplest of all models and basses on the analysis of observed data; and require a relatively coarse resolution data input. Universal Soil Loss Equation (USLE) (Cohen et al., 2005; Wischmeier & Smith, 1978) and its revised version RUSLE (Nyakatawa et al., 2001; Renard et al., 1997) are the examples of statistical or empirical models which need long term rainfall measurements measured in short duration. Conceptual models represent the catchment as a sequence of internal storage system and include the general description rather than the specific details of process interactions within the watershed under study. LASCAM (Viney & Sivapalan, 1999) is one of the examples of a conceptual models which uses daily rainfall as input. Physically based models use equations of conservation of mass and momentum for both sediments and flow, and usually require a large amount

of measurement data. OpenLISEM (Baartman et al., 2012; De Roo et al., 1996a) is an example of physically based models. Since the distinction of between the three types of aforementioned models is not sharp, there is a likely mix of modules from each of the categories during modeling applications (Merritt et al., 2003). Therefore, there is no single model which fits to all the scales and purpose of study and all models need calibration (Jetten et al., 1999). Furthermore it is not necessarily that the predictive quality of physically based models are always better than the empirical models (Jetten et al., 2003). However the advantage of physically distributed models is the fact that calibration is with known physical parameters and the detailed spatial information of many processes can be visible.

2.4   LISEM model

The Limburg Soil Erosion Model (LESEM) is a new physically based (De Roo et al., 1996a) hydrological and soil erosion model that has been developed by the Department of Physical Geography at Utrecht University and the Soil Physics Division at the Winard Staring Centre in Wageningen, the Netherlands, for planning and conservation purposes. The structure and principles of LISEM model were described elsewhere in many (De Roo & Jetten, 1999; De Roo & Offermans, 1995; De Roo et al., 1996a; Merritt et al., 2003) papers.
The main principle of LISEM model is based on (R. P. C. Morgan et al., 1998) European Soil Erosion Model (EUROSEM).

Rainfall, interception, surface storage in micro-depressions (surface roughness), infiltration, percolation, overland flow, channel flow, detachment by rainfall and through fall, detachment by overland flow and transport capacity of the flow are processes incorporated in LISEM model (De Roo et al., 1996a). LISEM does not require long hydro-meteorological records and it has widely been applied in many studies (Baartman et al., 2012; De Roo & Jetten, 1999; Hessel et al., 2003b; Jetten et al., 2003; Jetten et al., 2006; Kværnø & Stolte, 2012; Sheikh et al., 2010). The results from these studies reveal that there is a good agreement between the predictive values of LISEM and the actual measured values after calibration. LISEM is one of the first examples of a physically based model incorporating a raster geographical information system (De Roo et al., 1996a), which enables the model easy application in larger catchments, being user friendliness and allows remotely sensed data to be used than the other models, (for example, the empirical type of models). LISEM model includes soil and hydrological properties for modeling of the hydrological response of a watershed unlike the empirical model types which only include soil properties and relief (hence have no sense about flowing water).

 LISEM is easy to calibrate (De Roo et al., 1996b) and calibration could be done by comparing the output result of the model with the measured discharge and sediment data. But the user must have enough information about the parameters he/she is changing related to the real ground information in the study area. LISEM is sensitive to hydraulic conductivity and initial soil moisture content (De Roo & Jetten, 1999; De Roo et al., 1996b; Hessel et al., 2003b). Hydraulic conductivity (Ks) is the most sensitive variable with respect to discharge, whereas Manning's/random roughness (n) and transport capacity (g1) to the soil loss output. Therefore, the model can be calibrated by changing the multiplication factor of these variables. Changing the hydraulic conductivity, and the Manning's(n) values affect the maximum discharge and the occurrence time of the maximum discharge, respectively (Baartman et al., 2012). As LISEM a user friendly, for example, it allows the user to specify the simulation time, the beginning, the end time and the time step to which the output will be recorded.

2.4.1   LISEM inputs

Modeling of runoff and soil erosion by LISEM requires a large number of maps (Jetten, 2002) depending on the options selected in the interface (Figure 2-1). In general, approximately more than 25 maps in PCRaster format are required to simulate runoff and erosion using LISEM. These are rainfall ID, catchment morphology maps, land use maps, surface cover related maps, erosion related maps, infiltration related maps, and channel morphology maps (Appendix I). However, these maps can be generated from a few basic maps like digital elevation model (DEM), land use map, soil information from field observation and impermeable area maps (De Roo et al., 1996a; Jetten, 2002). Rainfall data either from multiple rainfall gauges as table format or from satellite as PCRaster format is also an input. Hence, LISEM has the ability to incorporate both the spatial and temporal variability of rainfall.

2.4.2 LISEM outputs

The main outputs of LISEM variables include runoff, infiltration and soil erosion (erosion and deposition sediment). These output variables can be in total sums or values at a desired time interval over the period that is used for the model to run. LSEM produces maps which show the spatial distribution of soil erosion, infiltration and runoff at a desired time intervals during the simulation. The model is also capable to produce hydrographs and sediment graphs for the selected rainfall events under study. Since LISEM is able to produce detailed spatial distribution of soil erosion and runoff maps, it helps planners where to install conservation measures to guard the landscape and prevent erosion. During simulation the user is able to see the summary of the time series simulation results including the hydrograph at the selected outlet point. The latest versions (for example version 1.56) also allow visualizing the map and the hydrograph in the same interface while running the model (Figure 2-2).
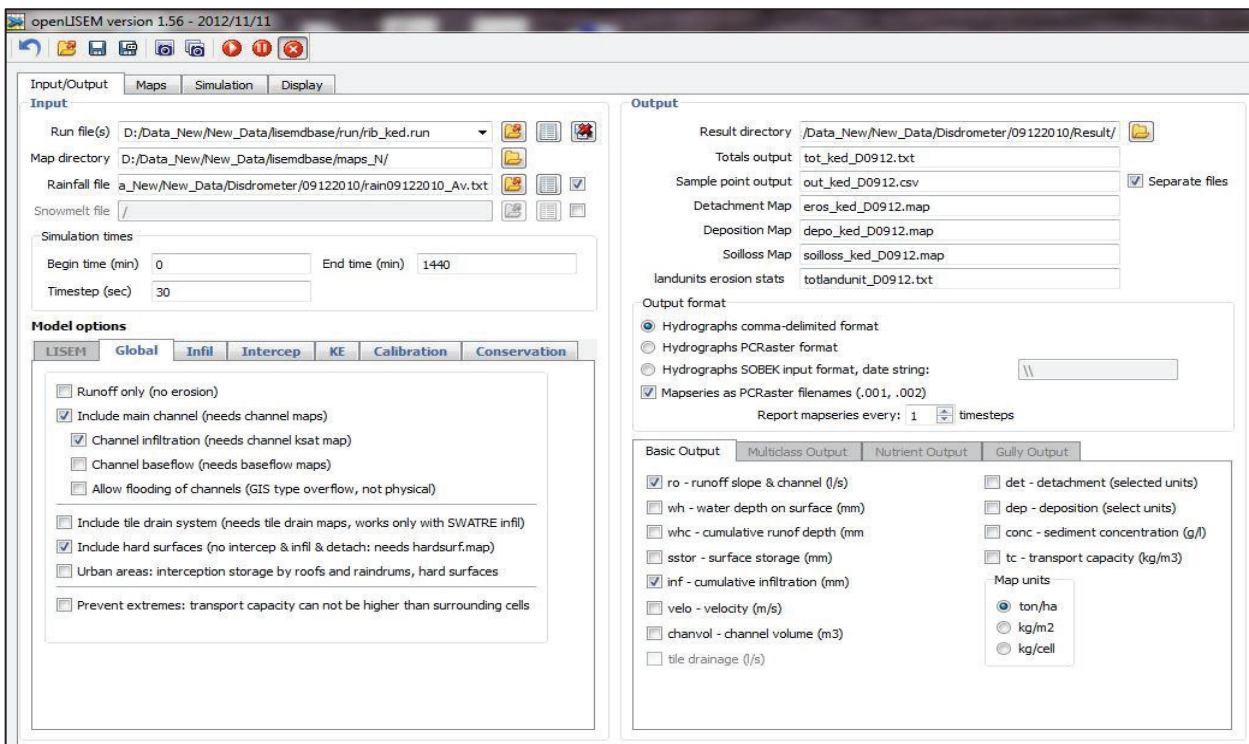
Figure 2-1: LISEM interface.
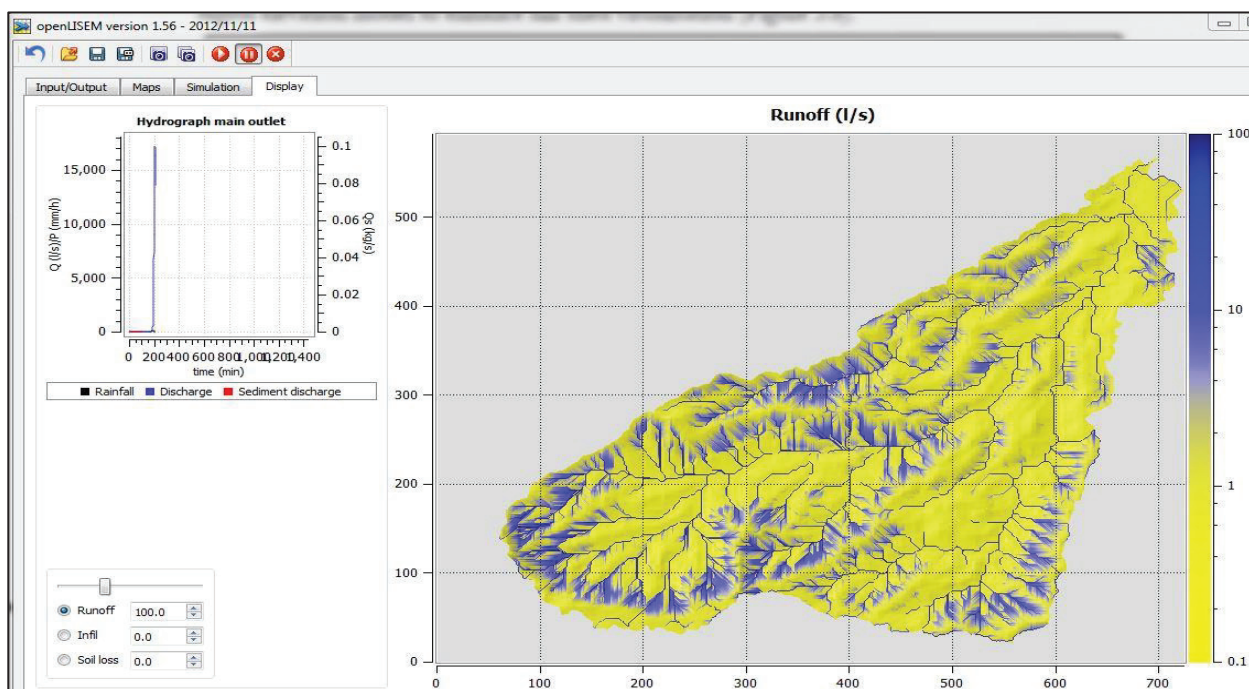
Figure 2-2: LISEM display interface.

3. MATERIALS AND METHODOLOGY

In this chapter first the study area (section 3.1) will be introduced followed by a description of rainfall data (section 3.2) and the detailed descriptions methodology used conduct the research process. The overall conceptual framework of the research process and the general data sets used for the study are shown in Figure 3-1.
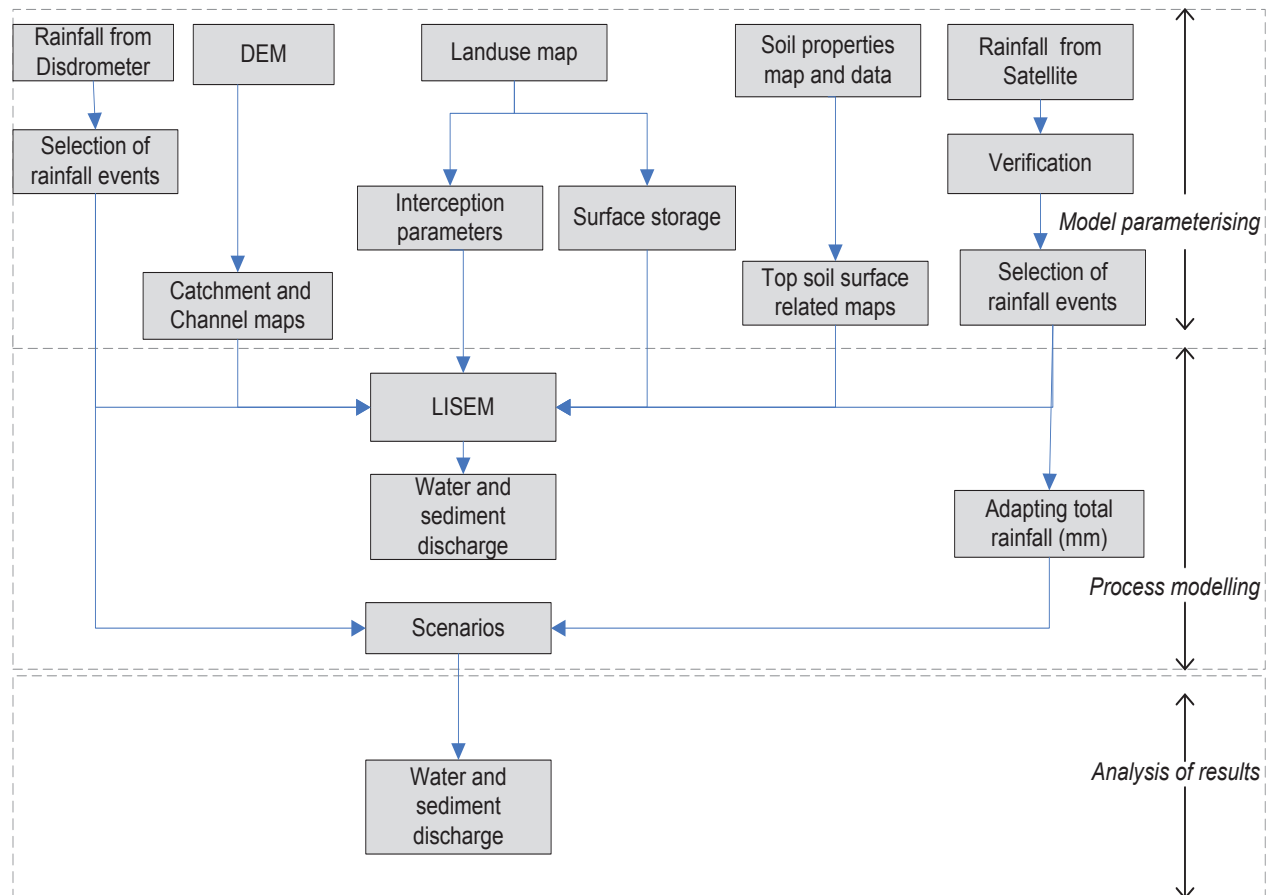
Figure 3-1: Conceptual frame work of the study.

3.1 Study area

The Cape Verde (Figure 3-2) is a mountainous archipelago composed by 10 islands of volcanic origin, located at about 500 km from the west most point of African continent (Dakar, Senegal), in the North Atlantic Ocean. Geographically, the Cape Verde islands are located between 15.02N and 23.34W. Out of the ten islands, nine of them are inhabited. The total area of the archipelago is approximately 4,033 km².

The climatic condition of the country is arid to semi-arid. Since Cape Verde is located in the dry tropical zone, its mean daily air temperatures range from 24^0C in winter to 29^0C during summer months (Sánchez-Moreno et al., 2008). Rainfall amount strongly depends on relief and elevation above sea level and range from less than 100 mm annually at sea level to around 800 mm (Mannaerts & Gabriels, 2000) per year in the mountainous areas above 100 m.a.s.l. Rainfall is almost entirely concentrated in the months of August to October. Streams are not permanent and water flows only during the rainy season. According to Sánchez-Moreno et al., (2008), the soils in Cape Verde are young ranging in thickness from 0.2 m in high slopes to 1 m in the valleys. The rugged relief and immaturity of the soils made the soil in the catchment highly susceptible to erosion. Severe water erosion and the fragile nature of the

land surface cause tons of land to be washed away from the fields during the rainy season every year in Cape Verde (DESIRE, 2012). In addition, the low soil cover and inadequate agricultural practice on rain fed lands posed a major problem related to soil erosion and desertification. Santiago Island is the biggest and most densely populated island in the Cape Verde archipelago. It is found with geographic coordinate of Latitude: $14^0 54'02''$-$15^0 20'26''$N and Longitude: $23^0 25'44''$-$23^0 46'59''$W, and has an area of 991 km².

The particular study area is Ribeira Seca catchment, located on the east side of Santiago Island (Figure 3-2). It is the largest catchment of the island having an area of 71.5 km² with geographic coordinate of Latitude: 15°01'55''N-15°07'40''N and Longitude: 23°32'05''W-23°38'40''W. High erosion rates during heavy rainfall events leading to soil degradation are common due to agricultural land use practices in the catchment (Evora Ferreira Querido, 1999). The area has a short rainfall season with high intensities. The annual average of rainfall varies between 200 to 650 mm. September is the wettest month and a harsh dry climate with little or no rain extends from mid-November to mid-July. Elevation in the catchment rages from 0 to 1,394 m.a.s.l. The main land uses (DESIRE, 2012) in the catchment are: subsistence (corn and beans) rain fed agriculture (83%), irrigated (5%) and forest (4%). From this it can be observed that vegetation cover is quite low, hence the susceptibility of the soil to erosion is high. The main on-site and off-site degradation processes are water and sedimentation, respectively. Major drivers for degradation are population growth, deficient information, insecure land tenure and lack of institutional mechanisms(DESIRE, 2012).
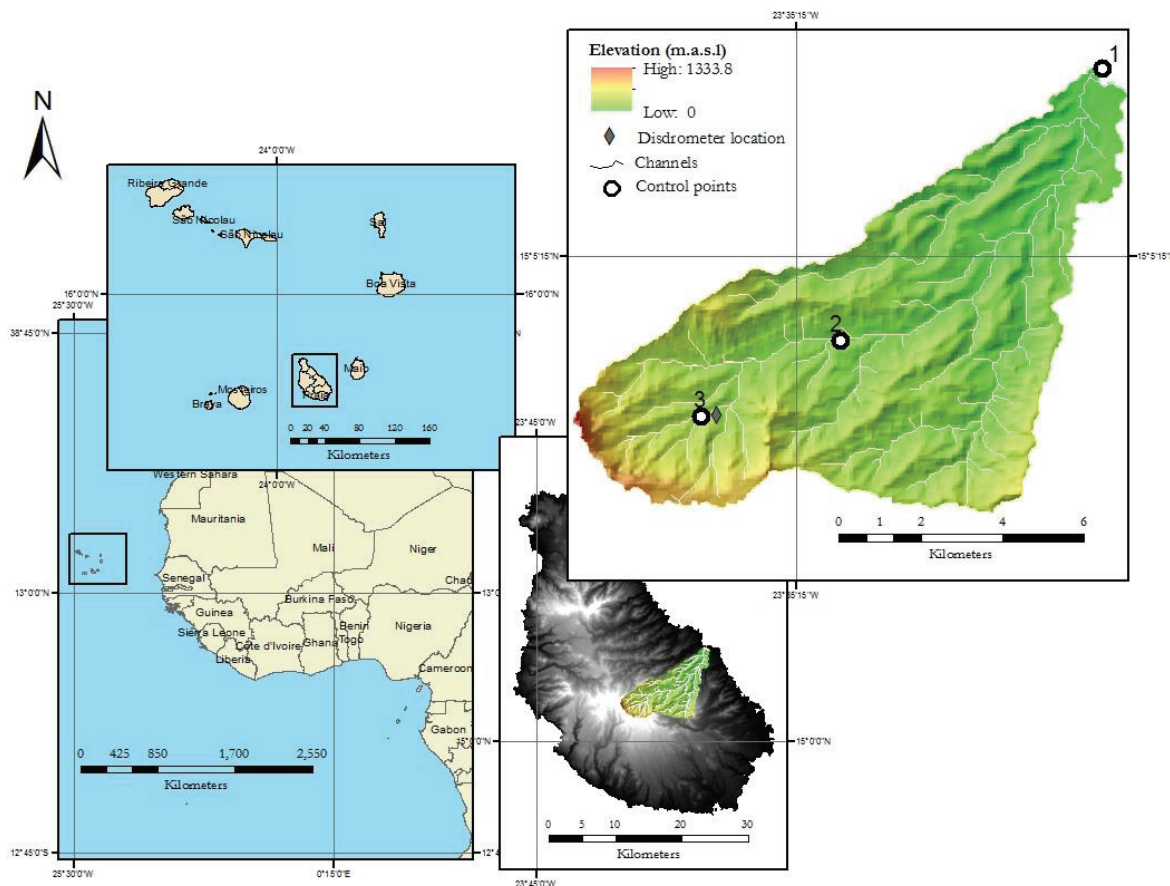
Figure 3-2: Study area; Continental Africa and Cape Verde (bottom left), Cape Verde with Santiago Island (top left), Santiago Island (DEM) with Ribeira Seca catchment (bottom right) and Ribeira Seca catchment with disdrometer and control points location (top right). Source: Sanchez-Moreno et al., (2012b).

3.2   Rainfall data

3.2.1   Ground based disdrometer rainfall

For ground based rainfall data collection, an OTT PARSIVEL (PARticle SIze and VELocity) disdrometer was installed (Sanchez-Moreno et al., 2012a) in Ribeira Seca catchment at a geographic location of $15^0 03'9.1''$N and

$23^0 36'17.7"W$ at an elevation of 321 m.a.s.l (Figure 3-2). The disdrometer collected rainfall intensity data from 1 of September 2008 until 16 of September 2010 using 3-minute time interval. The Parsivel is an optical sensor that emits a laser beam 30 mm wide, 180 mm long and 1 mm high (Loffler-Mang & Joss, 2000; Yuter et al., 2006). When a particle falls through the laser beam, the signal is interrupted decreasing the detection area for a fraction of time. From the reduction in area and the duration of the signal interruption, the diameter and velocity of the particles are detected. Yuter et al., (2006) noted that the disdrometer does not recognize the different particle sizes within a size interval. Hence, all particles detected within an interval are assigned the mean size for that interval. The OTT Parsivel disdrometer was selected due to its accuracy, data accessibility, portability and low cost operations as compared to similar devices (Loffler-Mang & Joss, 2000; Sanchez-Moreno et al., 2012a). Besides, a disdrometer has an advantage of measuring data directly related to raindrop distribution than traditional rain gauges.

Since data from disdrometer is available from 1 of September 2008 to 16 of September 2010, any comparisons with the disdrometer measurement discussed in this study refer to this time period only. In addition from 12 August 2010 to 18 August 2010, there was no disdrometer recorded data. To allow for rain depth comparisons with the 15 minutes satellite rainfall depth, the 3 minutes disdrometer intensity were aggregated (aggregating the 5 consecutive readings) to 15 minutes and converted to rain depth. Afterwards, 15 minutes rain depth were further aggregated to daily and compared with daily rain depth from rain gauge and satellite.

In order to compare the rainfall intensity measured at a single location by the disdrometer at 3 minutes interval with the satellite, two possible ways of bringing the high temporal resolution (3 minutes) intensity (mmh^{-1}) recorded by disdrometer to 15 minutes were studied. The purpose of bringing the intensity products from both sources to the same temporal resolution is to compare and prepare rainfall inputs (of the same temporal resolution) for OpenLISEM model.

The first way is to take directly the 3 minutes intensity values that correspond to every 15 minutes by ignoring the rest of the remaining values. This method seems to be the correct way in terms of time consideration since the rainfall intensity from MSGMPE at a particular time is a snapshot of that time. In other words, for instance, the intensity from MSGMPE say at 15 minute is not an average from 0 to 15 minute time period. It is an intensity estimated at that particular 15 minute time. In this sense, comparisons of the direct intensity belonging to every 15 minutes measurement from the disdrometer with that of MSGMPE seems to be realistic. However, this method excludes the other rainfall intensities contributing to the total rainfall depth that occurred in that particular event; therefore, it underestimates the rain depth (Table 4-8), which actually recorded in the real world. On top of this, the five events obtained based on event index (see section 3.3) which takes into account the total rain depth as one of the event characteristics. Therefore, direct taking of every 15 nth minutes reading is found to be unrealistic.

The second way is to aggregate the 5 consecutive 3 minutes intensity readings and make use of their average. Despite this method appears to be unrealistic in the exact time consideration, it takes into account the total rain depth occurred in any particular event. Hence, due to the aforementioned drawbacks of the first way, an aggregation of the consecutive 5 intensity (3 minutes) readings recorded by disdrometer and averaging them, was used to compare with the intensity from the corresponding MSGMPE for the five events. Rainfall intensity based comparisons is done for the five events due to the fact that these five events were the events with which their EVIs are > 0.5 and their measurement of rain depth from both (disdrometer and MSGMPE) were reliable.

3.2.2   Rain gauge measurements

Daily rainfall depth (mm) recorded data (Sanchez-Moreno et al., 2012a) measured with an automatic rain gauge at station San Jorge (located at 140m North West of the disdrometer) was used for comparison and verification. The daily rainfall depth measured by rain gauge from 1st of August 2008 to 31st of October 2010 covering the rainy season was used for additional verification of satellite estimate precipitation. The station is administered by the National Institute for Meteorology and Geophysics of Cape Verde (INMG). Since the rainfall depth from rain gauge is available on daily, the 3 minutes disdrometer and the 15 minutes MSGMPE rainfall intensity were converted to rain depth and aggregated to daily for comparison with rain gauge data.

3.2.3   Satellite based rainfall estimate

Rainfall intensity estimates were extracted from 1st of August 2008 to 31st of October 2010 from Meteosat Second Generation Multi-Sensor Precipitation Estimate (MSGMPE). MSGMPE data was downloaded through the DVB (digital video broadcasting)-based Ku-band broadcast service of EUMETSAT, using a data receiver located at ITC, The Netherlands (Jeniffer et al., 2010; Maathuis et al., 2006). The MSG data retriever tool developed by ITC takes into account the radiometric and geometric resolution of images. The general process taken for the analysis of both ground and satellite based rainfall data is shown in Figure 3-3.
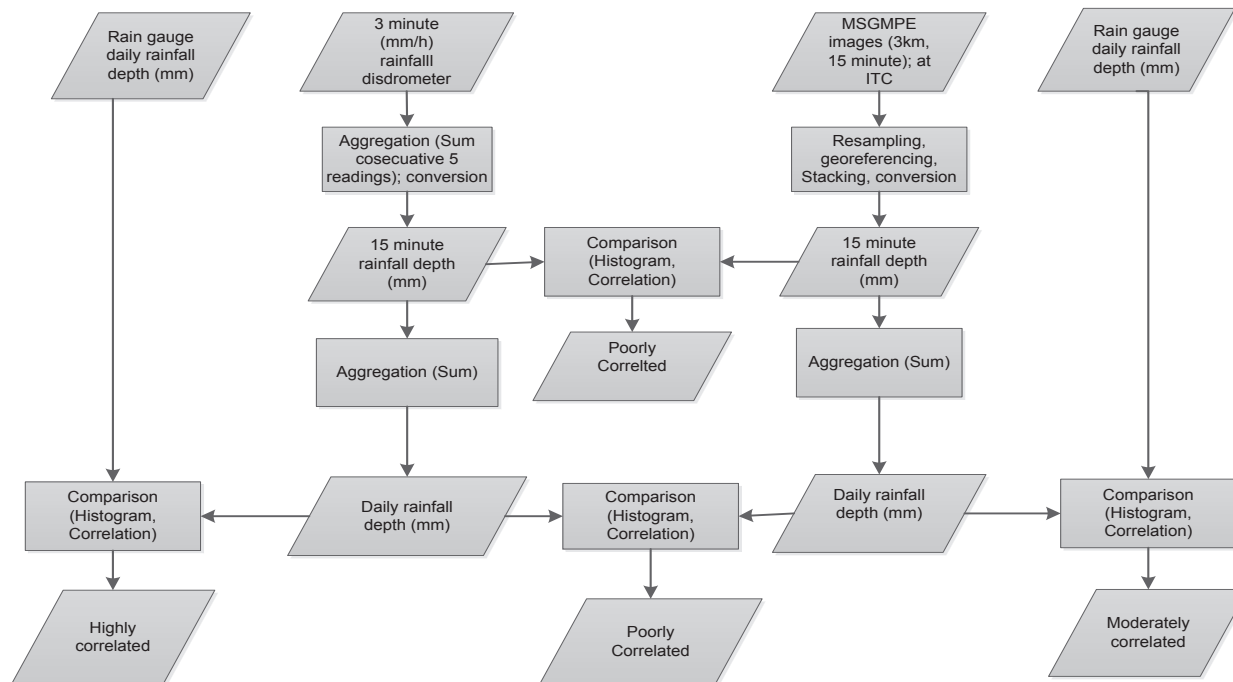
Figure 3-3: Flow chart of the rainfall analysis.

MSGMPE rainfall (mmh^{-1}) images (96) of 15 minutes temporal and 3 km spatial resolutions of global coverage were downloaded for every day. Afterwards, each image is cut-off to the areal extent of Santiago Island using the nearest neighbor resampling method (ILWIS v3.7.2). The cut-off is aimed at observing the spatial variability of rainfall over the island and the catchment. It is also further aimed at making ready the images for reliable extraction of rainfall intensity values of the pixel corresponding to the disdrometer location. During cut-off, the images are georeferenced to the geographic coordinate of Cape Verde and the spatial resolution is maintained constant for further processing. The resampled 96 images per day were stacked into one map using ILWIS v3.8 map list creating technique for automatic extraction of rainfall intensities. Finally, the 96 MSGMPE rainfall (mmh^{-1}) value corresponding to the disdrometer pixel location was extracted as table format and exported to excel for further time series comparison with ground rainfall depth measurement data. The extracted satellite data covers 269 days of the three years of the rainy season. For the remaining 7 days (15 to 21 of August 2009), there was no MSGMPE data at EUMETSAT.

Due to uncertainties (A. T. C. Chang & Chiu, 1997) related to satellite derived rainfall products, these products should be validated (Thiemig et al., 2012) before use as an input for any hydrological applications. Therefore, the goodness of satellite-based rainfall estimation has to be evaluated before use in runoff or erosion related modeling purposes. The performance of these satellite derived rainfall data are evaluated by direct comparison with the available ground based data measurements (Collischonn et al., 2008; Sandoval Gómez, 2007; Tapiador et al., 2012). In order to verify the MSGMPE estimated rainfall, a comparison with 15 minutes, daily, monthly and annual rainfall depths with ground rainfall data measurements was employed. To account for the time offsets between the Parsivel

disdrometer and the satellite measurements, the two data sets were brought to the same time and date during comparisons.

Rainfall (mmh^{-1}) measured at a single location by the disdrometer at 3 minutes interval was averaged to every 15 minutes (mm h^{-1}). Afterwards, both intensity products were converted to rainfall depths (mm) for comparison (Figure 3-3) on 15 minutes, daily, monthly and annual bases time series for the period 2008 to 2010 years. In order to account for spatial and timing offsets (Jeniffer et al., 2010; Maathuis et al., 2006; Sanchez Moreno et al., 2012b), average MSGMPE rainfall depth values of the nine (3 x 3 windows) pixel surrounding the location of the disdrometer were tested for some of the rainfall events. However, the result revealed that no improvement of the MSGMPE rainfall depths except slight changes of insignificant values. Therefore, the comparisons were done for the single-pixel corresponding to the disdrometer location. Correlations between ground and satellite rainfall data were performed by plotting rainfall time series (Table 4-3 to Table 4-6). The 15 minutes MSGMPE rainfall depth (mm) estimates were aggregated to daily totals and were compared to the catch of ground based rain gauge (San Jorge station) precipitation on daily basis (Figure 4-4). This comparison covers the full dates of the three rainy months (August, September and October) of the three years since there was data from both sources.

3.3 Selection of rainfall events

Runoff and soil erosion are closely related to rainfall in one way or another. For example, soil erosion is closely related to rainfall either through the detaching power of the rain drops or through contribution of rain to runoff. Therefore, modeling of runoff and soil erosion by event based models requires selection of rainfall event which gives a hydrological response. LISEM, an event based model requires selection of rainfall events from rainfall data analysis, which gives more response to the hydrological processes (Baartman et al., 2012). Classification of rainfall events depends on the objective of study (Kunkel et al., 1999) and events must have >5 mm total rainfall and >30 minutes total duration (Baartman et al., 2012). Furthermore, Baartman, et al., (2012) also proposed another method of selecting rainfall events which include three event characteristics having a vital effect on the hydrological response. These are: maximum precipitation intensity (P_{max}; mm h^{-1}), total precipitation (P_{tot}; mm) and total duration (T_{max}; min). The relationship of these three parameters is called event index (EVI). EVI = (P_{max} x P_{tot})/T, where a high EVI represents intense rain storm of short duration and high peak intensity, whereas a low EVI indicates rainfall events with low intensities but long duration. Therefore, in this study, the selection of events is based on these criteria; and rainfall events recorded by MSGMPE from 1st of August 2008 to 31st of October 2010 were used as baseline for events selection for further study.

3.4 Resampling (Interpolation)

The existing cell size of input raster maps (Appendix I) for the study was 20 x 20 m; whereas, rainfall data from MSGMPE is with 3 x 3 km spatial resolution. Therefore, the MSGMPE rainfall data for the selected rainfall events was down scaled (resampled) using two different resampling methods (ESSRI; Tolpekin & Stein, 2012). In resampling technique, the value of the output cell is determined based on the nearby or where the point falls relative to the center of cells of the input raster and the values associated with these cells. It is rare that an output cell center will align exactly (ESSRI) with any cell center of the input raster. The two techniques, described briefly below, after ESSRI, can be applied to continuous data, with nearest neighbor producing a blocky, inverse distance weighted producing smoother results. As described in section 3.2.3, global coverage of MSGMPE intensity images for the selected rainfall events were cut-off to the areal extent of Santiago Island using nearest neighbourhood interpolation method (Figure 3-3). Thereafter, the images were resampled to Ribeira Seca catchment areal extent with nearest neighbor and inverse distance weighted interpolation methods. A 20 m grid cell size and UTM coordinate system was used to bring to the same spatial resolution with the existing maps. Finally, the resampled images with the two techniques discussed below were exported to PCRaster.

3.4.1   Nearest neighbor interpolation

The nearest neighbor (NN) assignment does not alter the value of the input raster dataset cells; it is the resampling technique of choice for discrete (categorical) data. In nearest neighbor interpolation, the value of the nearest original (input cell) is assigned to the output raster. Since the output cell values remain the same, nearest neighbor interpolation should be used for nominal or ordinal data, where each value represents a class member or classification (such as land use, soil or forest type).

If the total amount of rainfall estimated by MSGMPE for the selected event over the entire catchment was lower than that measured by disdrometer, adapting the MSGMPE derived rainfall to disdrometer measured rain depth will be employed. Adapting is used in order to make the amount of rainfall that enters to the catchment from the two sources the same. The ratio factor (dividing the total rain depth from disdrometer by the total rain depth from MPE, and multiplying each cell of the MPE derived intensity by this factor) will be used for the selected event. Adapting MSGMPE estimated rain depth to disdrometer measured rain depth could be preferred due to the fact that disdrometer records the actual rain depth that occurred on the ground than MPE.

3.4.2   Inverse distance weighted interpolation

Inverse distance weighted interpolation (IDW) uses and implements the assumption that things that are close to one another are more alike than those that are farther apart. To predict a value for any unmeasured output raster cell, IDW will use the measured values of the input raster cell. Those measured values closest to the cell of the input raster will have more influence on the output cell value than those farther away. Thus, IDW assumes that each measured point of the input cell has a local influence on the output raster cell that diminishes with distance. Hence, IDW weighs the points closer to the prediction location greater than those farther away and smoothens the output surfaces.

In order to use IDW, evrey15 minutes MSGMPE intensity pixel center was converted to points using ILWIS v3.7.2. Then, these point centers of pixels were interpolated using IDW to an areal extent of the catchment, exported to PCRaster as ASCII format and converted to PCRaster format. In the same manner as discussed in section 3.4.1, adapting/correcting of MSGMPE derived rain depth that was interpolated by using inverse distance to disdrometer measured rain depth was employed.

3.5   Open LISEM model

Currently, an open source OpenLISEM version 1.59 is available. Many papers (De Roo & Offermans, 1995; De Roo et al., 1996b; De Roo et al., 1996a; Jetten, 2002; Kværnø & Stolte, 2012) described the principles of LISEM in detail. Baartman, et al., (2012) noted that there is no catchment size limit for application of LISEM, but the cell size and time step should be less than one hectare and one minute, respectively. The grid cell size should be between roughly 5 x 5 and 100 x 100 m² due to certain empirical equations (Jetten, 2011). In the present study, LISEM was applied for soil erosion modeling of the Ribeira Seca catchment (71.5 km²).Grid cell size is one of the most arbitrary choices in spatial modeling; however, it determines most of the outputs in raster-based models (Jetten et al., 2003). Since runoff and soil erosion processes vary spatially, cell size should be used which takes into account this spatial variation (De Roo & Jetten, 1999). Because the existing data set from previous study (of Ribeira Seca catchment) that was used in this study has a 20 x 20 m pixel size, this grid cell size is chosen for running the model. It is also important to keep the cell size as fine as possible for small catchments to represent the spatial variability of the input parameters to the model. The prediction of the models is more accurate when the resolution is higher (fine grid cell size) but at the expense of time. The choice of time step length could depend on the grid cell size chosen (Hessel, 2005), where smaller cell sizes require smaller time steps. A good rule of thumb (Jetten, 2002) is to use simulation intervals of 0.2 to 2 seconds(s) times the grid cell size in meter (m). Hence, a time step of 30 seconds is chosen to run the model. The temporal resolution of the satellite derived rainfall is 15 minutes. The assumption here is the rainfall is homogeneous throughout the 15 minute time period and this temporal resolution is also fair enough to be used in erosion modeling by LISEM.

3.6   Runoff and soil erosion modeling inputs

Besides the high temporal and spatial resolution of rainfall input maps, Open LISEM requires four main groups (De Roo et al., 1996a; Jetten, 2002; Sanchez Moreno et al., 2012b) of input maps:

- maps related to relief and flow direction, which can be derived from DEM,
- maps related to soil surface characteristics and cover, that can be derived from land use or land cover, with roads and impermeable areas,
- maps related to hydraulic soil properties and strength properties which are linked to soil and/or land use maps, and
- maps of channel network with channel characteristics.

The maps related to hydraulic soil properties and soil strength properties which are usually linked to soil and/or land use maps were generated in four different ways by Sanchez-Moreno et al., (2012b). But for this study those soil maps generated by Kriging with External Drift (KED) was used. The reason is that those maps produced by KED follow the spatial trend(Sanchez Moreno et al., 2012b) of the map used as external drift (for example, soil depth follows the slope pattern and random roughness follows land use). The other input maps produced from the above four groups of maps (Appendix I) were obtained from previous study by Sanchez-Moreno et al., (2012b). Hence, the brief descriptions of the input maps summarized below were taken from that study.

"Relief related and flow direction maps were derived from a 90 meters resolution DEM from the Shuttle Radar Topography Mission (SRTM). Land use map was retrieved from a supervised classification of an ALOS-AVNIR image of June 2009. Impermeable areas were retrieved from previous study and the land use map classification. Soil type and soil characteristics were obtained from previous study and field observation. Table 3-1 shows the summary and statistics of the soil parameters measured in the catchment.

Soil properties measurements were done using purposive sampling in three campaigns and conducted between September and October of 2008 to 2010. A total of 79 saturated hydraulic conductivity (Ks) points were retrieved, out of which 75 points were within Ribeira Seca catchment and 52 points for additional soil properties such as cohesion, random roughness and porosity. Infiltration was measured in the field with mini disk infiltrometer and saturated hydraulic conductivity was calculated. During the first and second campaign, 49 and 21 infiltration points were measured respectively. Furthermore, 23 core samples were taken for laboratory that were used to measure porosity. Cohesion was measured with a torvane tester in the field. For each sampling point, four measurements spaced between 0.5 and 1 meter were taken randomly and averaged. Soil depth was measured with tape along roads and slope cuts. In flat areas, it was measured using the pocking pole method, with an iron bar driven into the soil. Surface roughness was measured in the field using chain method."

Table 3-1: Statistical information for soil parameters mapped (Sanchez Moreno et al., 2012b).

Parameter	Minimum	Maximum	Mean	Standard deviation	No of samples
Porosity (%)	0.03	0.60	0.30	0.19	52
Cohesion (kPa)	0.98	11.00	5.70	2.74	52
Soil depth (mm)	100	1000	30	22	52
Roughness C_{rr}	0.50	7.00	2.40	1.40	52
Random Roughness (RR)	0.07	1.00	0.35	0.20	52
K_s field (mm h^{-1})	0.20	69.30	15.60	14.80	70
K_s laboratory (mm h^{-1})	0.86	41.30	12.10	16.20	8
K_s total (mm h^{-1})	0.20	69.30	15.10	14.90	78
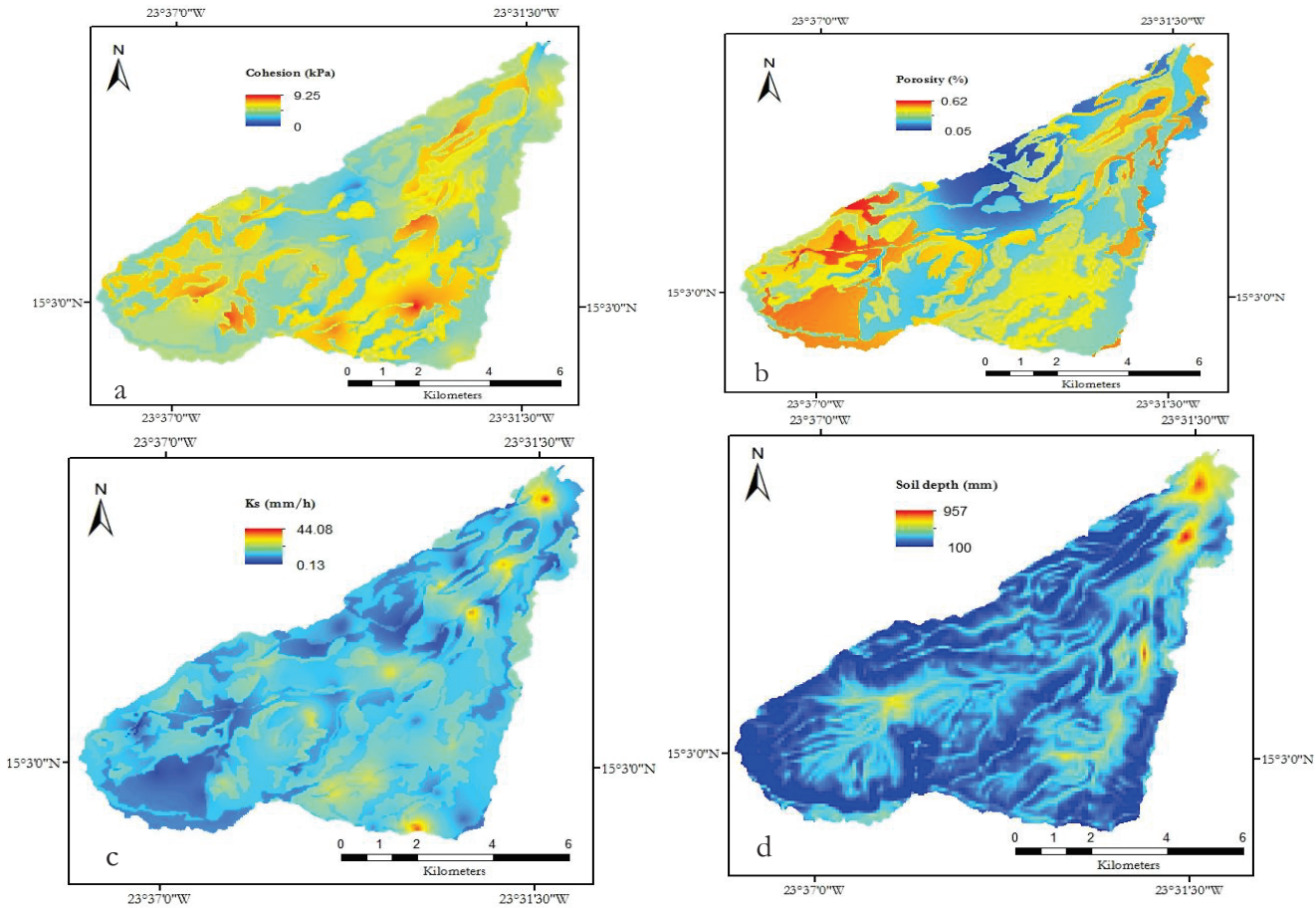
Figure 3-4: Four main soil input maps (among many others) produced by Sanchez-Moreno et al., (2012b): a) cohesion (kPa), b) porosity (%), c) soil depth (mm) and d) saturated hydraulic conductivity (mmh[-1]).

Figure 3-4 shows soil cohesion, porosity, depth and saturated hydraulic conductivity input maps (among many others) produced by previous study. The soil maps were produced by Kriging with external drift (KED) and have statistical information shown in Table 3-1. The lowest porosity was observed mostly at the north-west corner of the catchment. This area is also with lowest cohesion and low soil depth, hence susceptible to erosion. Areas with high porosity were mostly mapped at the bottom south-west areas. This area corresponds to low cohesion and relatively high soil depth; therefore, less susceptible to runoff and erosion as well.

3.7   Rainfall scenarios on runoff and soil erosion processes

The simulation of erosion from both homogeneous rainfalls and that of satellite derived rainfall as inputs to the LISEM for the selected event is to observe the effect of spatial variability of rainfall on runoff and sediment discharge over the catchment. The homogeneous rainfall was measured by disdrometer at a single location in the catchment; whereas, the spatially variable rainfall was estimated by MSGMPE over the entire catchment.

For the fact that the total amount of rainfall that enters into the catchment is one of the main factors influencing the hydrological response process of a given watershed, total rainfall has to be the same from two different sources to make reasonable comparisons of infiltration, runoff and soil erosion process. The total rainfall (46 mm) over the entire catchment estimated by MSGMPE for the selected event was lower than that measured by disdrometer (66 mm). Hence, adapting the MPE estimated rainfall to the disdrometer measured rainfall depth was employed. To do so, a ratio factor (total amount of disdrometer rain depth/total amount of MSGMPE derived rain depth over the full catchment) correction factor was used to bring the total amount of rain that enters to the catchment from both sources the same and to make realistic comparisons of the results. Therefore, the MSGMPE derived rainfall (mmh[-1]) was multiplied by a factor of 1.435 (66/46). Adapting MSGMPE rainfall estimate to disdrometer measurement is preferred due to the fact that disdrometer measured the actual rain depths that occur on the ground. Then, the model was run with the same amount of rainfall from both sources

4.   RAINFALL RESULTS AND DISCUSSIONS

4.1   Rain gauge, Disdrometer and Satellite rainfall comparisions

Figure 4-1 presents the daily rainfall depth (mm) measured by the automatic rain gauge (located at 140 m North West of the disdrometer), Parsivel disdrometer and estimated by MSGMPE comparison for the rainy season between 2008 and 2010 years. But it is worth mentioning the disdrometer measured data exists only from 1 of September 2008 to 16 of September 2010. Hence, any result and discussion related to disdrometer holds for this time period only.

Even though different authors have used different thresholds, rainfall amount of 0.1mm per day was often used as a threshold value to define a dry day due to the usual precision of rain gauges measurements (Ceballos et al., 2004; Mathugama & Peiris, 2011). In this study, despite days with rainfall < 0.8 mm were not reported by rain gauge, taking into account the underestimation of daily rain depth by MPE and the minimum amount of daily rain depth that can be recorded by rain gauge (Martin-Vide & Gomez, 1999), a threshold value of 0.1 mm per day is used to define a dry day.

Therefore, taking the minimum daily rain depth to be 0.1mm, the rainy season onset occurred in the first weeks of August (ranging from 1st to 5th of August); and offset reported on in the last weeks of October (ranging from 24th to 31st of October) between the three years from the three measurements. Hence, the onset and offset of the rain season is not largely varied from year to year. For example, in 2009, the rain onset from rain gauge was on 5th of August with rain depth of 10.3 mm; whereas from disdrometer, it was on 1st of August with rain depth 0.2 mm and that from MPE on 4th of August with rain depth of 0.4 mm daily precipitation. For the same year (2009), the offset rain day was on 28th of October as measured by rain gauge and disdrometer; and on 29th of October as estimated by MPE.

Table 4-1 shows the number of days with rain per month and per season, number of days with rain >5 mm per month and per season, and the maximum daily raifall per month and per season that are recorded by rain gauge, disdrometer and estimated by MPE for the rainy season between 2008 and 2010. The maximum daily rainfall indicates the highest average daily rainfall recorded within the month and season. For all the three years period, the total number of rain days (daily rain >0.1 mm) reported by rain gauge was 79, by disdrometer was 130 and by MPE was 79. However, for the same time period the total number of days with rain > 5 mm reported by rain gauge was 62, by disdrometer was 42 and by MPE was 36. Despite the highest number of days with rain, the disdrometer reported lower number of days with rain > 5 mm than the rain gauge, implying the ability of disdrometer to record small intensities. Further more, though data from MPE was available for the full period, the total number of days (36) reported with rain > 5 mm were the lowest among the three measurement methods. In each of the three measuring methods September is the month which resulted in higher rainfall mean per month. For example a mean per month rainfall of 11.2 mm from rain gauge, 17.0 mm from disdrometer and 8.2 mm from MPE was obtained for September 2010 (Table 4-1). This implies that September is the wettest month of the rainy season than other months. 2010 is the year with the highest rainfall mean pear season from the three measuring methods.
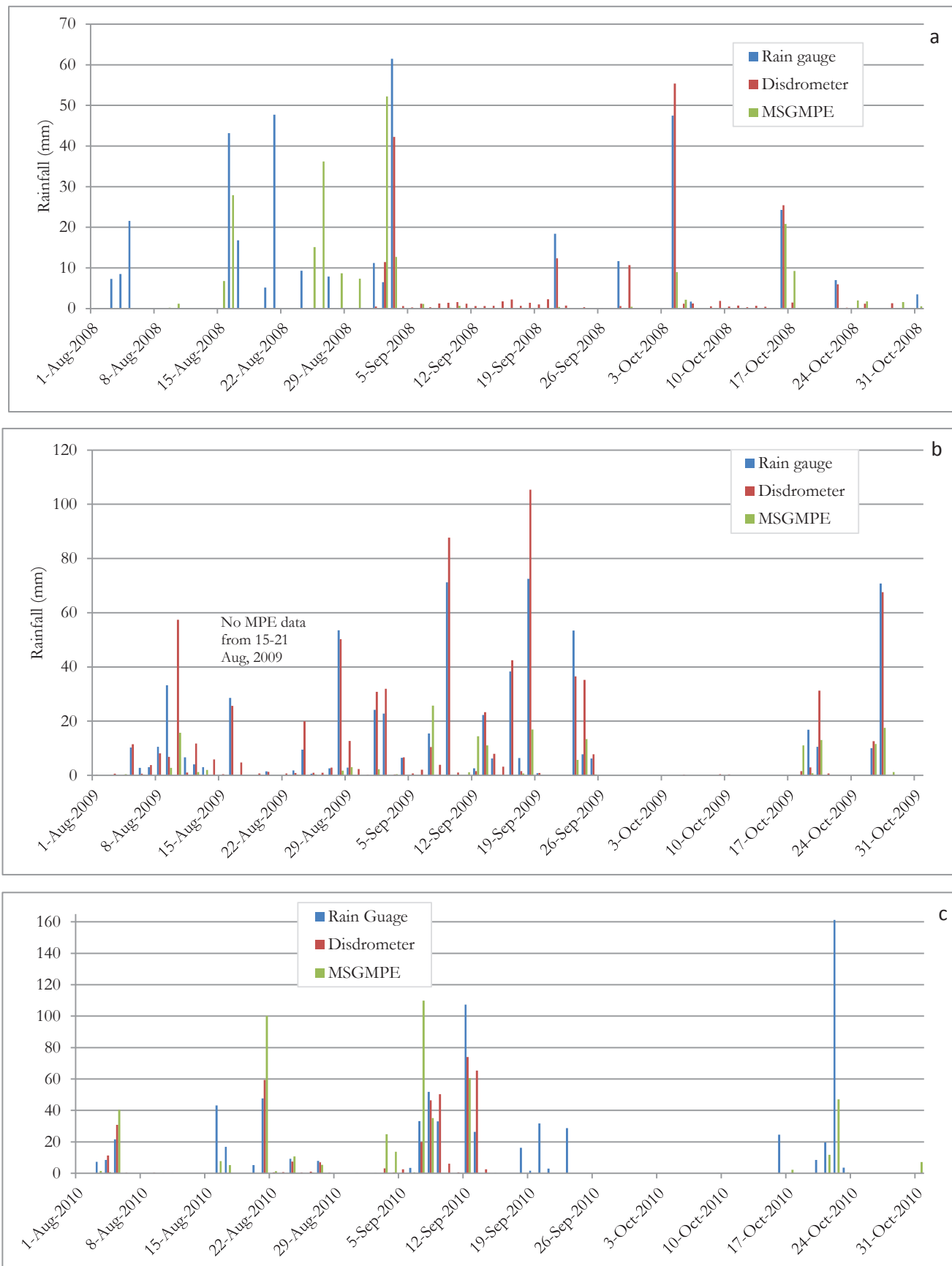
Figure 4-1: Daily rainfall depths (mm) measured by rain gauge, Parsivel disdrometer and estimated by MSGMPE comparisons of: a) 2008, b) 2009 and c) 2010 years.

Table 4-1: Number of days with rain and number of days with rain >5 mm, and mean rainfall (mm) per month and per season that are recorded by rain gauge, disdrometer and estimated by MPE between 2008 and 2010.

Year	Period	Days with rain			Days with rain > 5 mm			mean (mm) per month & season		
		Gauge	Disdrometer	MPE	Gauge	Disdrometer	MPE	Gauge	Disdrometer	MPE
2008	Aug	9	*	9	9	*	6	5.4	*	3.3
	Sept	5	27	7	5	4	2	3.6	3.3	2.3
	Oct	5	17	9	3	2	3	2.7	3.2	1.5
	Season	19	44	25	17	6	11	3.9	3.2	2.4
2009	Aug	16	27	10	7	10	1	5.6	7.5	1.2
	Sept	15	21	14	13	12	6	11.9	14.7	3.1
	Oct	4	9	6	4	3	4	3.5	3.8	1.8
	Season	35	57	30	24	25	11	7.0	8.6	2.1
2010	Aug	9	15	11	9	5	6	5.4	5.0	5.6
	Sept	11	14	7	8	6	5	11.2	17.0	8.2
	Oct	5	*	6	4	*	3	7.1	No	2.2
	Season	25	29	24	21	11	14	7.9	10.1	5.3

* No disdrometer record data.

Table 4-2: Maximum daily rainfall (mm), total rainfall (mm) and percentage (%) of maximum daily rainfall per month and per season that are recorded by rain gauge, disdrometer and estimated by MPE between 2008 and 2010. In bold the highest percentage of the maximum daily rainfall per season from the three measurement methods.

Year	Period	Maximum daily rainfall (mm)			Total rainfall (mm)			% of maximum daily rainfall		
		Gauge	Disdrometer	MPE	Gauge	Disdrometer	MPE	Gauge	Disdrometer	MPE
2008	Aug	47.7	*	36.2	167.5	*	103.7	28.5	*	34.9
	Sept	61.5	42.3	52.2	109.3	98.8	67.9	56.3	42.8	76.9
	Oct	47.5	55.4	20.8	84.0	98.8	47.2	56.5	56.1	44.1
	Season	61.5	55.4	52.2	360.8	197.6	218.7	17	**28.0**	**23.9**
2009	Aug	53.5	57.4	15.7	174.6	232.6	27.8	30.6	24.7	56.5
	Sept	72.5	105.4	25.7	356.7	441.7	92.5	20.3	23.9	27.8
	Oct	70.8	67.6	17.5	108.1	117.8	55.2	65.5	57.4	31.7
	Season	72.5	105.4	25.7	639.4	792	175.6	11.3	13.3	14.6
2010	Aug	47.7	59.5	100.2	167.5	120.2	173.4	28.5	49.5	57.8
	Sept	107.4	74.1	109.9	336.5	271.7	245	31.9	27.3	44.9
	Oct	161.3	*	47.1	217.5	*	68.3	74.2	*	69.0
	Season	161.5	74.1	109.9	721.5	391.9	486.7	**22.4**	18.9	22.6

*No disdrometer record data.

Table 4-2 presents the maximum daily rainfall (mm), total rainfall (mm) and percentage of maximum daily rainfall per month and per season that are recorded by rain gauge, disdrometer and estimated by MPE between 2008 and 2010. Figure 4-2 shows as an example the the maximum daily precipitation (mm) per month (August, September and October) for the year 2010 that is estimated by MPE over Santigo Island, Ribeira Seca catchmrent and at a location of disdrometer.

It is observed that the larger the number of rainy days doesn't necessary translate to high rainfall depths from the three measuring methods. For example in 2010, the number of rain days reported by rain gauge was 25, whereas, the total rain depth was 721.5 mm (highest of all the years). This is attributed to the fact that a single daily strom can contribute up to 74.2 % (Oct, 2010 from gauge), 57.4 % (Oct, 2009 from disdrometer), 76.9 % (Sept, 2008 from MPE) of the monthly rainfall depth, and can contribute up to 22.4 % (2010 from gauge), 28.0 % (2008 from disdrometer and 23.9 % (2008 from MPE) of the season (Table 4-2). Except August 2010, MSGMPE underestimated the total rain depth per month as compared to rain gauge and disdrometer measurements (Figure 4-3). In general 2010 was the year with the maximum total rainfall recorded by rain gauge and estimated by MSGMPE. The lower totl rainfall for this year recorded by disdrometer could be due to the lack of data for 15 days of September and the full days of October 2010. Hence, 2008 was the year with lowest total rainfall and 2010 was the year with highest total rainfall recorded by the three measuring methods.
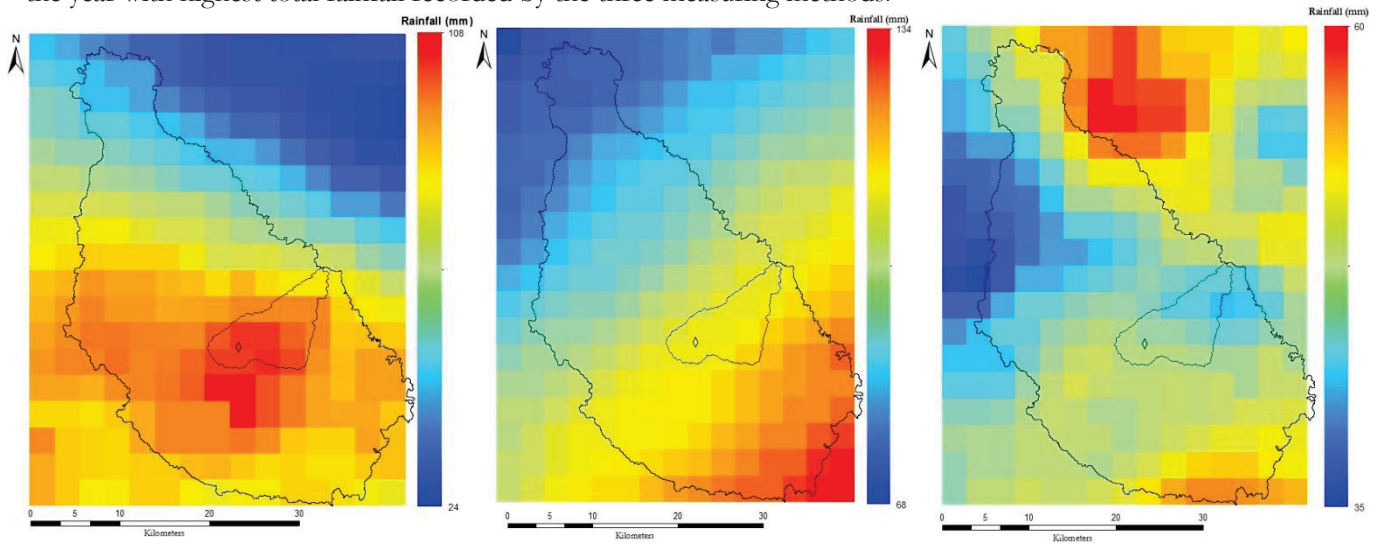
Figure 4-2: Daily precipitation (mm) estimated by MSGMPE (3 km cell size) over Santiago Island and Ribeira Seca catchment: a) 08122010 b) 09072010 and c) 10222010 events.
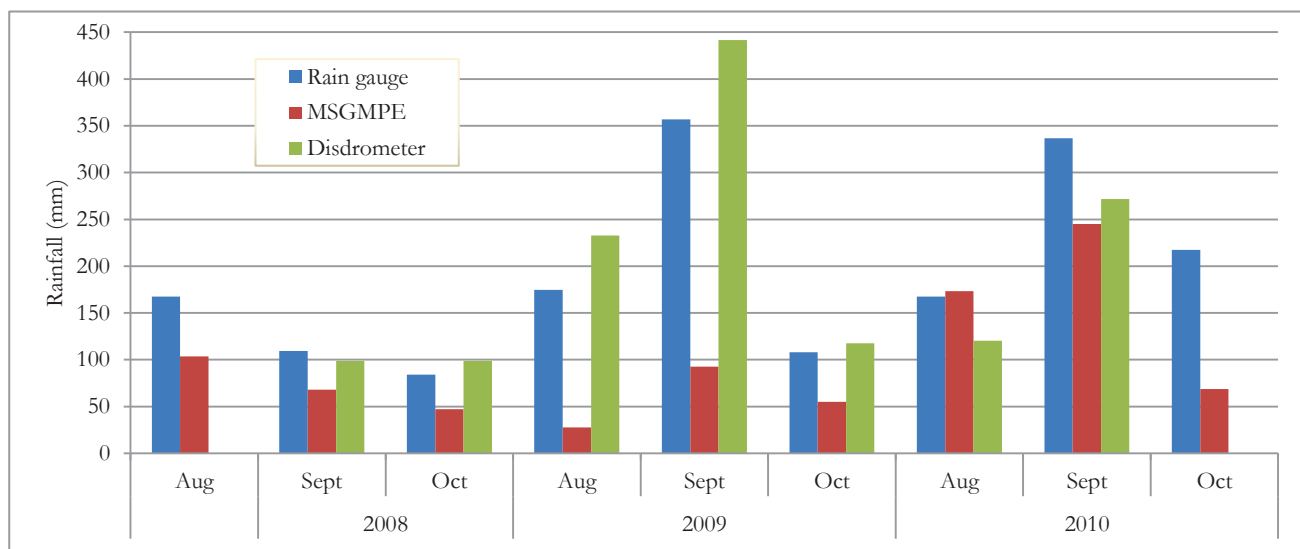
Figure 4-3: Monthly total rainfall (mm) measured by rain gauge, disdrometer and estimated by MSGMPE comparison for the rainy season between 2008 and 2010 years.

4.1.1　Rain gauge versus disdrometer rainfall

Figure 4-4 shows the comparison of the daily rainfall depth measured by the automatic rain gauge data from station San Jorge and disdrometer for the period from 1 of September 2008 to 16 of September 2010 (this time is the time period for which the measurement from disdrometer exists). Figure 4-5 presents the scatter plot of the daily rain depth measured by rain gauge and disdrometer for the same time period. The two data sets show a good correlation with coefficient of determination of R^2 equals about 0.79.
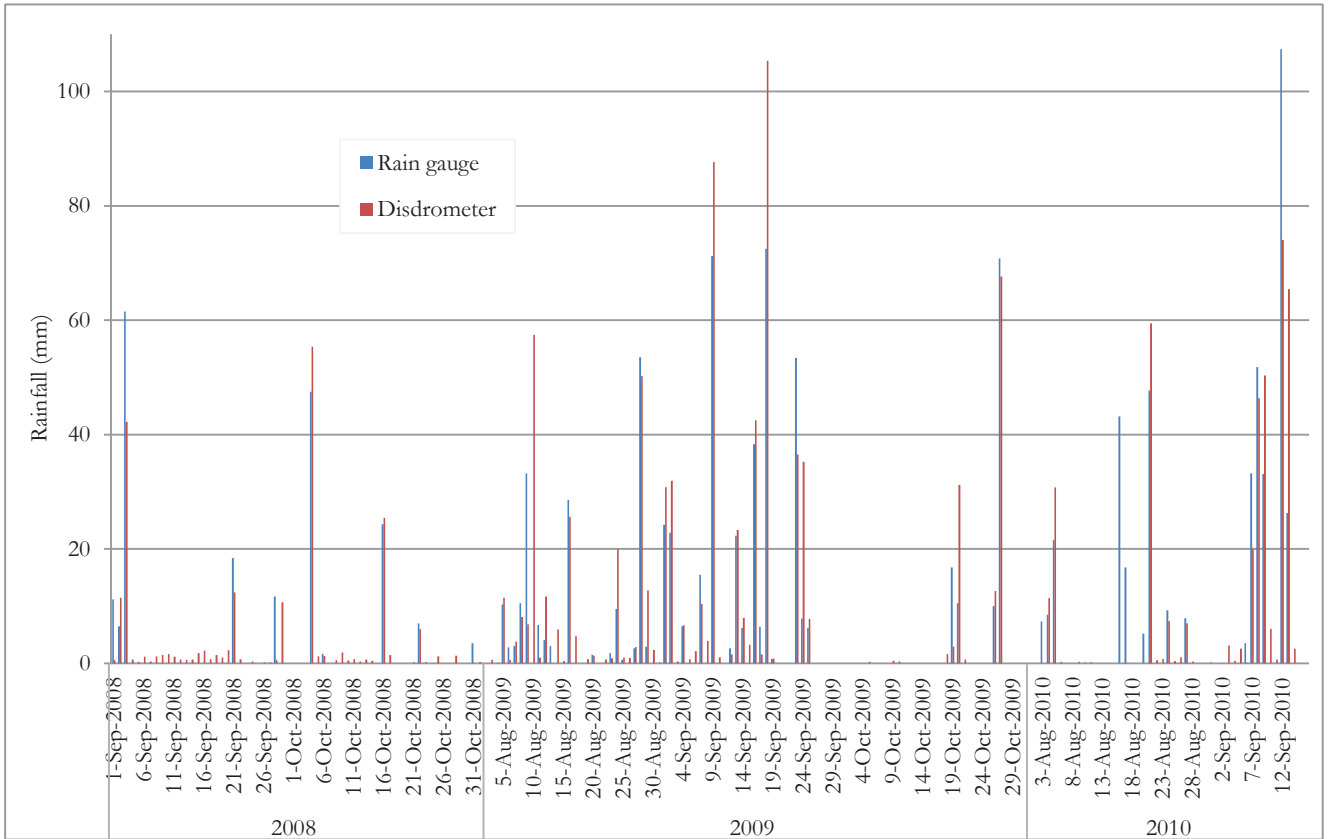
Figure 4-4: Daily rainfall depths (mm) measured by rain gauge and Parsivel disdrometer from 1 of September 2008 to 16 of September 2010.
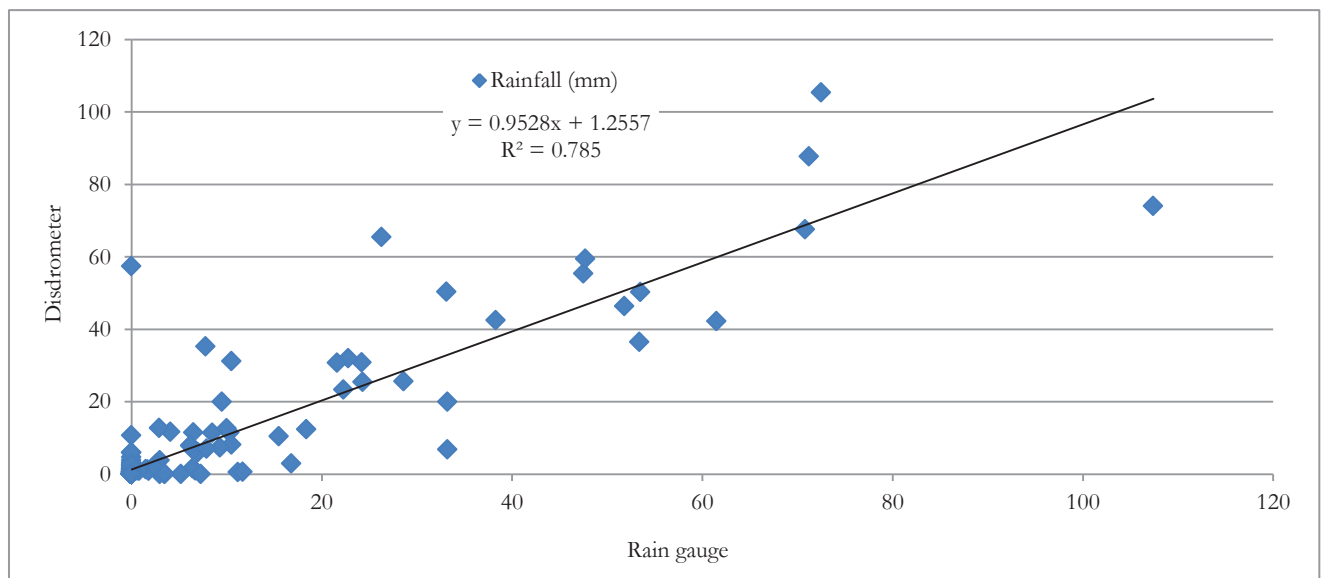
Figure 4-5: Scatter plot of daily rainfall depth measured by rain gauge and Parsivel disdrometer for the period from 1 of September 2008 to 16 of September 2010.

From Figure 4-4 and Figure 4-5, it can be observed that the disdrometer recorded a number of days with rain that were reported dry by rain gauge. For the same time period, disdrometer recorded 130 rain days with rain depth greater than 0.1mm; whereas, only 59 days with rain were reported by rain gauge.

Sanchez Moreno et al., (2012 a) explained two main reasons that could cause the difference in rainfall depths reported. These are the ability of the disdrometer to detect small particles other than rain drops resulting in false small intensities, and the manual recording by visual inspection of the rain depth measured by the rain gauge a day after the event occurs. Since the reading of the recorded rain by rain gauge takes a day after the event occurs evaporation has also a considerable effect as the area is semi-arid. There were only 29 days reported by rain gauge with daily rain depth values greater than that recorded by disdrometer. However, 102 days with which the total amounts of daily rain depth recorded by disdrometer having higher values than that recorded by rain gauge were reported. Nevertheless a high correlation with coefficient of determination (R^2) equals 0.87 for 2008, 0.77 for 2009 and 0.8 for 2010 were obtained from the daily rain depth yearly comparisons (Appendix II). Other studies (Petan et al., 2010; Sanchez-Moreno et al., 2012a; Ulbrich & Miller, 2001) also found a good agreement between disdrometer and rain gauge precipitation measurements.

4.1.2   Rain gauge versus satellite rainfall

Figure 4-6 shows the aggregated 15 minutes MSGMPE precipitation estimates to total daily depths (mm) compared to the catch of the ground based rain gauge precipitation. Unlike the comparison of rain gauge and disdrometer, rain gauge and satellite comparison covers the full dates of the three months (August to October) for the period from 2008 to 2010. However, there was no MSGMPE data at EUMETSAT from 15-21 August 2009. A rain depth of less than 0.1mm from both sources was eliminated during comparisons.

Figure 4-7 presents the scatter plot of the daily rain depth measured by rain gauge and estimated by MSGMPE from 1 of August 2008 to 31 of October 2010. The two data sets show an overall correlation with coefficient of determination of R^2 equals 0.24. As can be seen from Figure 4-6, besides underestimation of total daily precipitation by MSGMPE, there are days with rain depth reported by rain gauge but not by MSGMPE and vice versa. In contrast to the comparison with the disdrometer, except its underestimation, MSGMPE captured 15 more days with rain than that of the rain gauge. However, the result shows that rainfall depths estimated by MSGMPE were found to be in a reasonable agreement with the total rainfall measured using a rain gauge at San Jorge station. The daily plot of monthly comparisons revealed a correlation with better coefficient of determination except August and September 2009 (Table 4-3). Daily plot of yearly comparisons (Table 4-4) also showed a good correlation except for the year 2009. The poor correlations (daily plot of monthly and yearly comparisons) obtained in 2009 could be attributed mainly to the extreme underestimation of the rainfall depth by MSGMPE. 2010 was found to be the year with the best ($R^2 = 0.46$) correlation of total rain depth in both monthly and yearly comparisons of daily values.

Table 4-3: Statistical daily based monthly comparison of Rain gauge and MSGMPE data.

Year	Month	R^2	Total precipitation (mm)		Remarks
			Rain gauge	MSGMPE	
	Aug	0.34	167.5	103.7	
2008	Sept	0.87	109.3	67.9	
	Oct	0.53	84.0	47.2	
	Aug	0.02	174.6	27.8	**
2009	Sept	0.02	356.7	92.5	
	Oct	0.65	108.1	55.2	
	Aug	0.59	167.5	173.4	
2010	Sept	0.71	336.5	245	
	Oct	0.93	217.5	68.3	

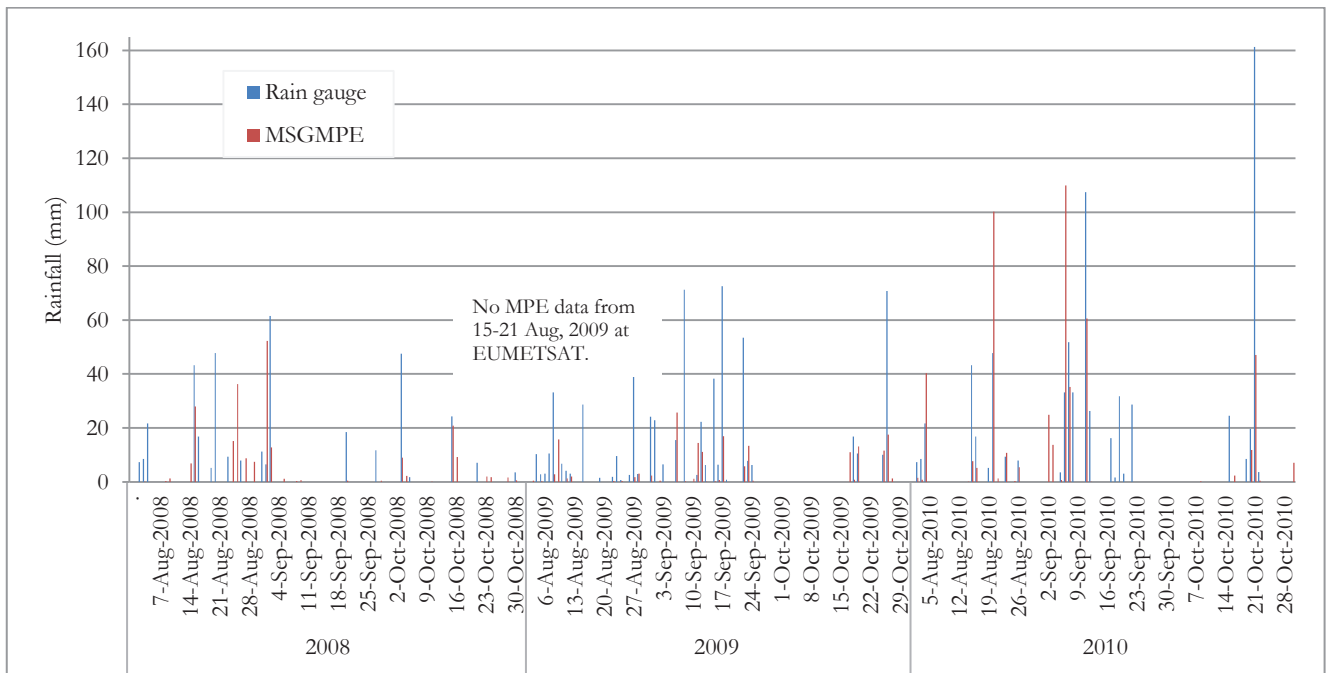**No MSGMPE data from 15-21 of August 2009 at EUMETSAT

Figure 4-6: Daily rainfall depths (mm) measured by rain gauge and estimated by MSGMPE from 1 of September 2008 to 31 of October 2010.
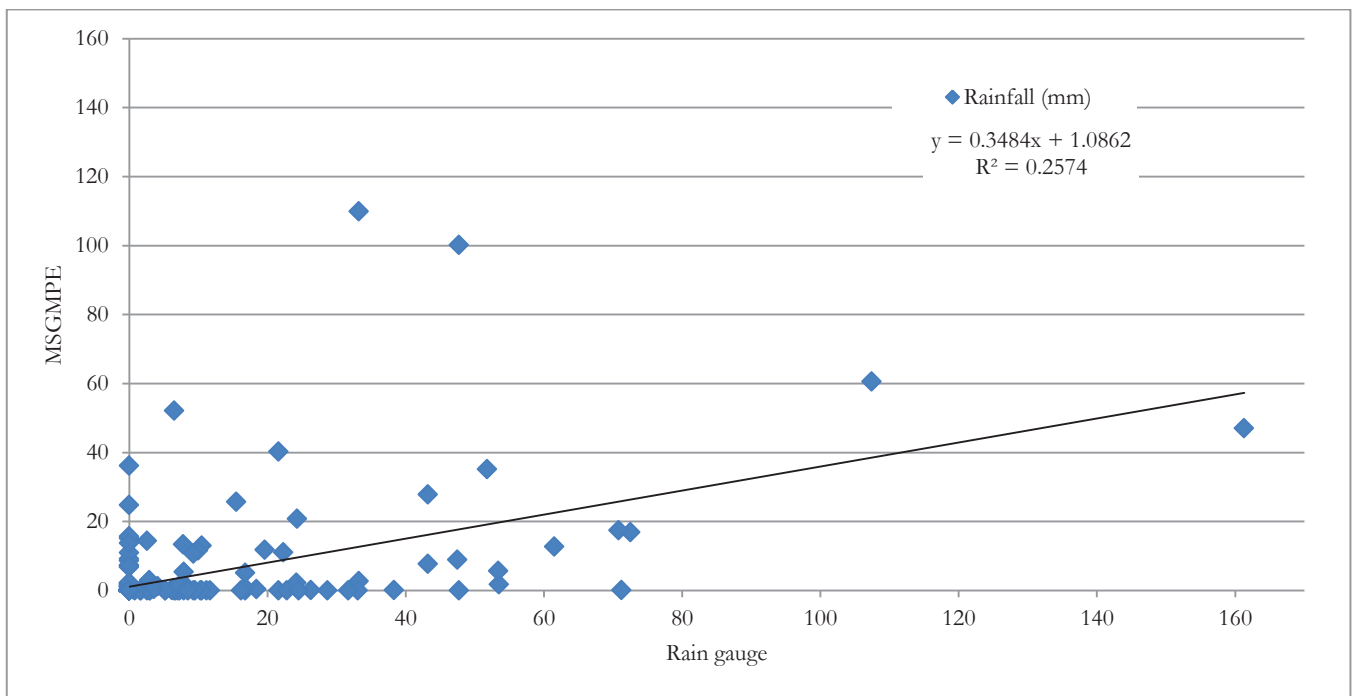
Figure 4-7: Scatter plot of daily rainfall depth measured by rain gauge and estimated by MSGMPE from the period 1 of August 2008 to 31 of October 2010.

Table 4-4: Statistical daily based yearly comparison of Rain gauge and MSGMPE data.

Year	R^2	Total precipitation (mm)		Remarks
		Rain gauge	MSGMPE	
2008	0.35	360.8	218.7	
2009	0.27	609.4	175.6	**
2010	0.46	721.5	486.7	

** No MSGMPE data from 15-21 of August 2009 at EUMETSAT

4.1.3 Parsivel disdrometer versus satellite rainfall

The main problem with the validation of precipitation estimate from satellite is the lack of suitable independent reference or base data. This is due to the fact that the data for validation are usually not available at appropriate either spatial or temporal resolution, or both (Heinemann, 2003). In this study, MSGMPE was verified with rainfall measurements from disdrometer which has a better temporal resolution (3 minutes). Hence, a time series comparisons of the rainfall depth measured by Parsivel disdrometer and that of MSGMPE were employed. However, the comparisons were done for the period 1 of September 2008 to 16 of October 2010 due to the availability of disdrometer measured rainfall data.

On 15 minutes temporal resolution (15 minutes based daily plot), correlations with a maximum coefficient of determinations with R^2 equals 0.14 (09212008 event) for 2008, 0.35 (09232009 event) for 2009 and 0.26 (08052010 event) for 2010 were obtained. The poor correlation could be due to the fact that rainfall is derived from radiation (based on cloud top temperature), hence the algorithm used (Ebert & Manton, 1998; Jeniffer et al., 2010; Salvador et al., 2013) and the atmospheric layer under the precipitating clouds determine the amount of rainfall estimated by MSGMPE on the ground. However, the disdrometer and Rain gauge are also not perfectly correlated, while they are only 140 m apart. This shows that the rainfall at ground level is very variable, and a 3x3 km satellite image may probably not be able to capture this. So the estimated amounts are much lower because of the cloud top temperature algorithms that may not explain all precipitation, but the scatter may be the result of high variability at ground level.

Figure 4-8 presents the daily total comparisons of the rain depths estimated by MSGMPE and measured by disdrometer. The results show that MSGMPE underestimated rainfall depth values in almost all the days except a few days, where it either overestimate or predicted about same value as Parsivel disdrometer measurement. The overall daily rain depth correlation comparison over the three years revealed a coefficient of determination R^2 equals 0.26 (Figure 4-9).

On top of its underestimation of the total amount of precipitation, MSGMPE captured a considerable less number of rain days than the Parsivel disdrometer. Nevertheless, a good correlation was obtained on daily basis monthly comparisons, and a reasonably good coincidence between rain days. The daily plot of monthly comparisons revealed a correlation with better coefficient of determination (with R^2 >0.4) except September 2009 (Table 4-5). August 2010 was the month with the best correlation (R^2 =0.96) obtained; whereas, September 2010 was with low correlation. On top of the underestimation of MSGMPE, the low correlation of this month could be attributed to the short day comparisons (only 16 days out of 30). Daily values of yearly comparisons (Table 4-6) also showed a good correlation except for the year 2009. 2010 was the year with the best correlation (R^2=0.57) obtained; hence, most of the five events selected for further study were from this year (see section 4.2).
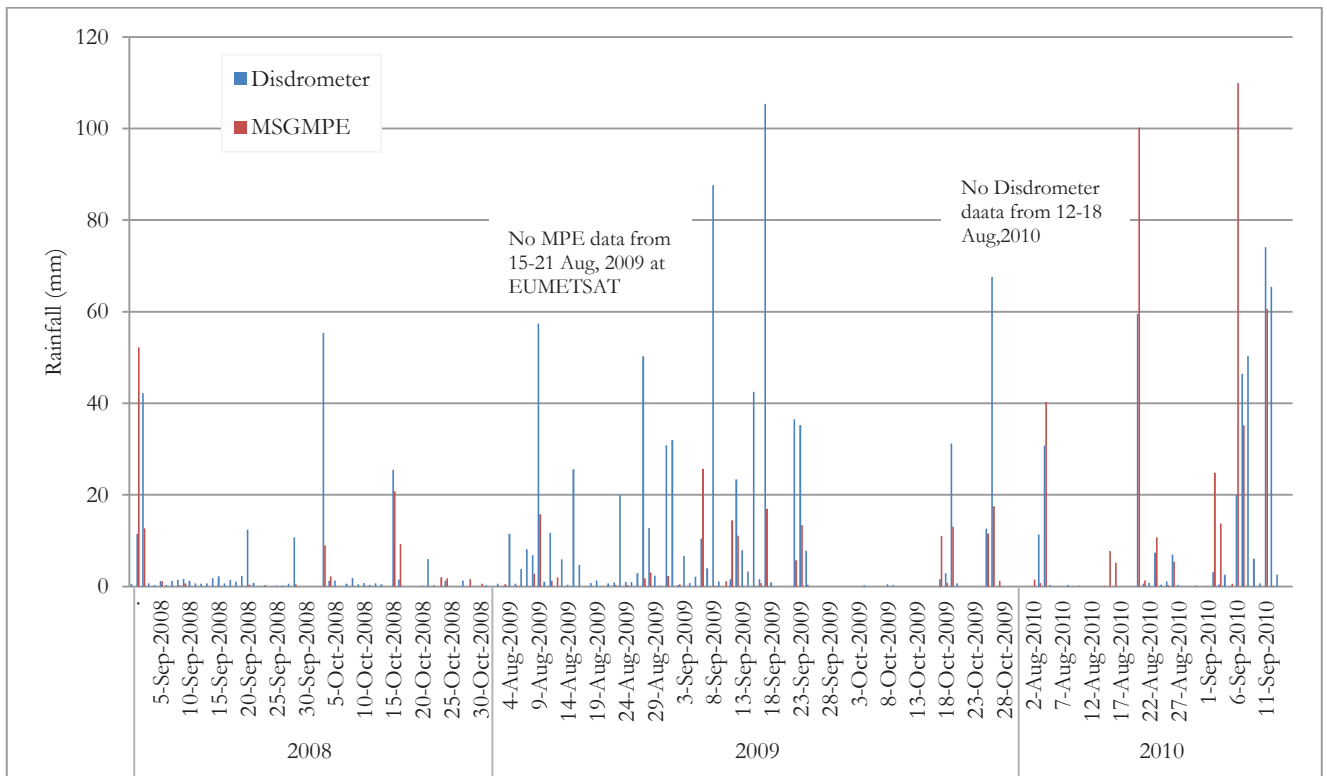
Figure 4-8: Average daily rainfall depths (mm) measured by disdrometer and estimated by MSGMPE from 1 of September 2008 to 16 of September 2010.
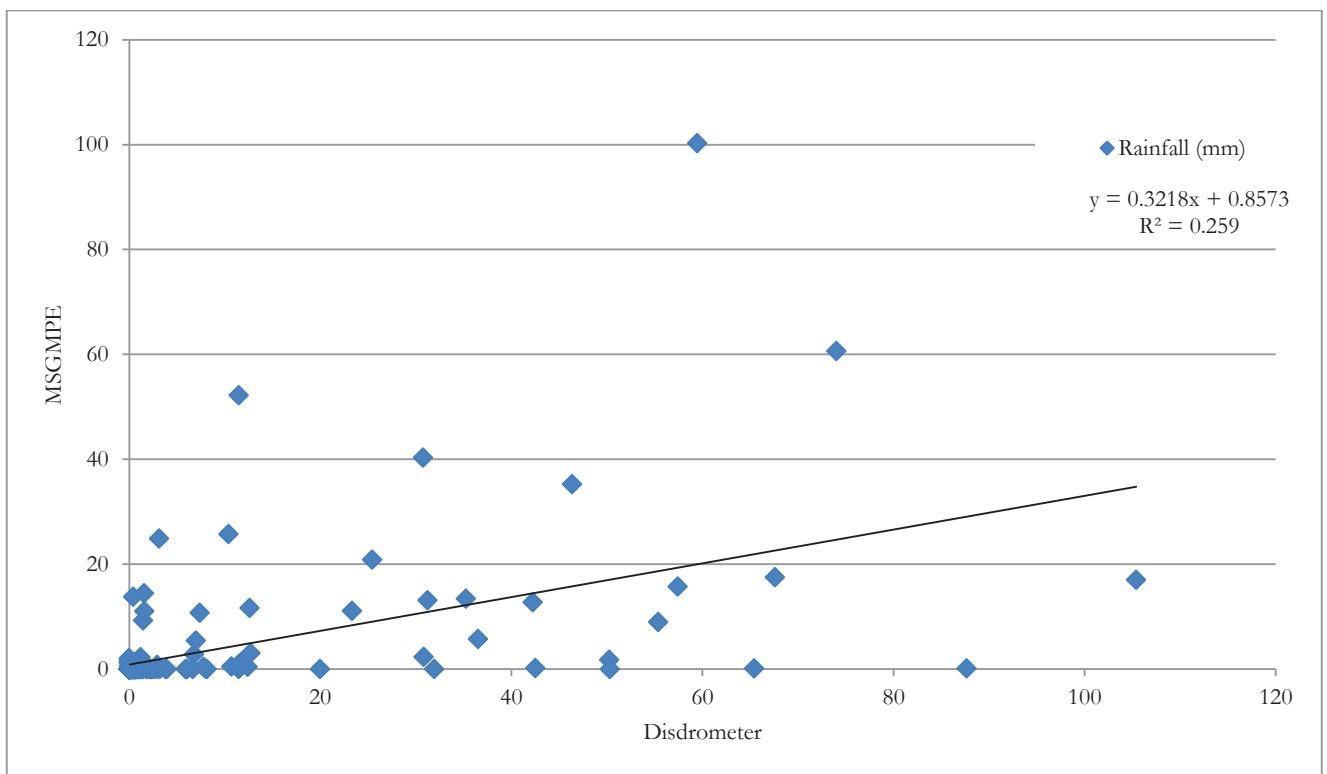
Figure 4-9: Scatter plot of daily rainfall depth (mm) measured by disdrometer and estimated by MSGMPE from 1 of September 2008 to 16 of September 2010.

Table 4-5: Statistical daily based monthly comparison of disdrometer and MSGMPE data.

Year	Month	R^2	Total precipitation (mm)		Remarks
			Disdrometer	MSGMPE	
2008	Sept	0.90	98.8	67.9	
	Oct	0.41	98.8	47.2	
2009	Aug	0.53	232.6	27.8	**
	Sept	0.02	441.7	92.5	
	Oct	0.71	117.8	55.2	
2010	Aug	0.96	120.2	173.4	*
	Sept	0.37	271.7	245.0	

**No MSGMPE data from 15-21 of August 2009 at EUMETSAT
*No Disdrometer record from 12-18 of August 2010

Table 4-6: Statistical daily based yearly comparison of disdrometer and MSGMPE data.

Year	R^2	Total precipitation (mm)		Remarks
		Disdrometer	MSGMPE	
2008	0.52	197.6	218.7	
2009	0.28	792.1	175.6	**
2010	0.57	391.9	297.04	*

**No MSGMPE data from 15-21 of August 2009 at EUMETSAT
*No Disdrometer record from 12-18 of August 2010

4.2   Rainfall events

MSGMPE has taken as a base line/leading for selection of events. Based on Baartman et al., (2012) criteria of rainfall event selection described in section 3.3, a total of 36 rainfall events from MSGMPE were recorded between 1 of September 2008 and 31 of October 2010 covering the rainy season. Among the 36 events, 25 of them fall within the period in which the corresponding measurement from disdrometer exists. However, only 20 (out of 25) events coincide with events with rainfall depths of > 5 mm that were measured by disdrometer. Since a high EVI results in high hydrologic response (Baartman et al., 2012), an EVI of 0.5 is arbitrary chosen as a lowest base line criteria for further selection of events. Among the remaining 20 events, 7 events resulted in EVIs greater than 0.5. Furthermore, even though the event indices of the other two (09022008 and 09182009) events were > 0.5, their measurements of rainfall by either of the two methods (disdrometer or MSGMPE) were not reliable. In event 09022008, the disdrometer measurement was unreliable (redundancy of measurement time and data) and in event 09182009, MSGMPE extremely underestimated the total rainfall. Hence, five events with EVI > 0.5 and distinct event characteristics were obtained.

Table 4-7 presents the 5 events with distinct event characteristics in terms of total precipitation, maximum peak intensity, and total duration having EVI greater than 0.5 that were recorded by MSGMPE between 2008 and 2010 years. The peak rainfall refers to the maximum intensity value of the pixel corresponding to the disdrometer location for each event; whereas, the total rainfall refers to the rain average total rain depth over the entire catchment. It should be noted that the peak rainfall (maximum intensity) over the entire catchment could be different from the intensity recorded at a location of the disdrometer. Furthermore, this peak intensity may represent the value of a single pixel or less than a single pixel over the entire catchment.

Table 4-7: Five events with event characteristics (total rainfall, peak rainfall and total duration) with EVIs > 0.5 obtained that were recorded by MSGMPE between 2008 and 2010.

Event Characteristics	09082010	08212010	09122010	08052010	10162008
Total rainfall (mm)	32.1	88.0	46.0	32.3	20.3
Peak rainfall (mmh^{-1})	29.2	29.7	24.8	15.6	14.3
Total duration (min)	150	420	225	225	525
Event Index (EVI)	6.25	6.22	5.07	2.23	0.55

Table 4-8 shows the total precipitation (mm) measured by disdrometer (with two ways of bringing the 3 minutes intensity to 15 minutes time, aggregated after converted to depth) compared to that estimated by MSGMPE for the five events, and the correlation of 15 minutes based intensity comparisons (with two ways of bringing the 3 minutes disdrometer record to 15 minutes). The comparisons were done over the period of length where there is measurements from both sources exist, but taking MSGMPE reading period as leading. The 'direct' refers to taking of every one 3 minutes intensity reading that corresponds to every 15nth minutes record; whereas, the 'average' refers to averaging the five consecutive 3 minutes intensity readings recorded by disdrometer, in order to bring to 15 minutes time. This is done for the purpose to compare with MSGMPE and to make ready for LISEM input at the same temporal resolution. The direct taking of the 3 minutes disdrometer intensity reading that corresponds to every 15 minutes underestimated the total rain depth of the respective events, except one (09082010). But in reality, there is rain depth recorded by disdrometer on the ground. Therefore, the intensity with the averaging technique was used for LISEM input for the selected event. The coefficient of determination R^2 stands for the 15 minutes based comparisons correlation of intensity estimated by MSGMPE and recorded by disdrometer (with two ways of bringing the 3 minutes intensity to 15 minutes time). In both cases the correlation is very poor with a maximum of R^2 equals 0.17 and 0.21 in direct and averaging, respectively. Despite the poor correlation obtained in both cases, the coefficient of determination obtained from comparisons of the averaging method resulted in a better coefficient of determination per each respective event than the direct method. It is worth mentioning the fact that the peak rainfall (maximum intensity) over the entire catchment could be different from the intensity recorded at a location of the disdrometer. Furthermore, this intensity may represent the value of a single pixel or less than a single pixel over the entire catchment.

Table 4-8: Total precipitation comparisons that is measured by disdrometer (with the direct taking every one 3 minutes intensity reading that corresponds to every 15 minutes and averaging the 5 consecutive 3 minutes readings to bring to 15 minutes time) and estimated by MSGMPE for the five events (over the total duration as shown in Table 4-7).

Events	Precipitation (mm)			R^2	
	Disdrometer		MSGMPE	Direct	Average
	Direct	Average			
10162008	15.3	24.9	20.3	0.01	0.02
8052010	16.6	27.3	32.3	0.17	0.21
8212010	38.8	56.7	88.0	0.01	0.01
9082010	17.4	17.0	32.1	0.02	0.19
9122010	63.5	66.0	46.0	0.02	0.01

Table 4-9 presents the five events (having EVI > 0.5) that were recorded by MSGMPE between 2008 and 2010 years compared in terms of event characteristics (total rainfall, peak rainfall and total duration) to their corresponding five events that were measured by disdrometer.

The peak rainfall from MSGMPE refers to the maximum intensity value of the pixel corresponding to the disdrometer location for each event; whereas, the total rainfall refers to the rain average total rain depth over the entire catchment. In the case of disdrometer, the total rainfall and peak intensity refer to the results obtained from averaging method of bringing the 3 minutes intensity to 15 minutes intensity. In all the events the EVI from the disdrometer measurements were found to be in order of higher values than the one recorded by MSGMPE per each respective event except the 09082010 event. This is attributed to the fact that either the peak rainfall (mmh^{-1}) from disdrometer is higher or the duration of the event is shorter. It is also observed that not only the peak rainfall and duration but also the total amount of rainfall determines the selection of events based on EVI. For example, in 09082010 events, though peak rainfall from disdrometer is higher than from MSGMPE, the EVI is lower. This is due to the lower in total rainfall from the disdrometer than the MSGMPE total rainfall even though the duration is the same for both. Therefore, this suggests that the combination of maximum intensity, total rainfall and event duration determines the selection of events.

Table 4-9: Comparison by event characteristics (total rainfall, peak intensity and total duration) of the five events that were recorded by MSGMPE (between 2008 and 2010 with EVI > 0.5) with their corresponding events that were measured by disdrometer (with averaging method of bringing the 3 minutes intensity to 15 minutes).

Event characteristics	09082010 Event		08212010 Event		09122010 Event		08052010 Event		10162008 Event	
	Disd.	MPE	Disd.	MPE	Disd.	MPE	Disd.	MPE	Disd.	MPE
Total rainfall (mm)	17.0	32.1	56.7	88.0	66.0	46.0	27.3	32.3	24.9	20.3
Peak rainfall (mmh^{-1})	33.9	29.2	61.0	29.7	119.6	24.8	51.4	15.6	47.2	14.3
Total duration (min)	150	150	420	420	180	225	195	225	270	525
Event index (EVI)	3.84	6.25	8.24	6.22	43.83	5.07	7.20	2.23	4.35	0.55

Disd. = Disdrometer

4.2.1 Event 09122010 (September 12, 2010)

Figure 4-10 shows the hyetograph of rainfall (mmh^{-1}) per 15 minutes and total duration comparisons of disdrometer measured and MSGMPE estimated rainfall for the event 09122010 among the five events with EVI > 0.5. This event is selected due to its high EVI from MSGMPE, has higher total rainfall amount that are close to each other from both measurement methods with short duration as compared to the other remaining four events (Table 4-8). Note also that though the plotting time (Figure 4-10) is the same for both measurements, the actual duration of the events is different.

Table 4-10 shows the event characteristics comparisons for the selected 09122010 event in terms of total rainfall, maximum intensity, total duration and EVI that were measured by disdrometer and estimated by MSGMPE. The total rainfall for MSGMPE was the result of the average rain depth over the entire catchment and the peak rainfall (mmh^{-1}) was the maximum intensity of the pixel value found over the entire catchment for this event. Both the peak intensity and total rainfall depth from disdrometer are higher than that estimated by MSGMPE. Furthermore, the total duration of the rain storm from disdrometer was shorter (180 minutes) than the storm from MSGMPE (225 minutes). Hence, the higher peak intensity and total rainfall with shorter duration of the storm from disdrometer resulted in the higher EVI (43.83) than the EVI (5.07) form MSGMPE.

Even though the total rainfall amounts from both sources are close, their difference is still significant (20 mm) to make difference in infiltration, runoff and erosion processes. It is apparent that the total amount of the rainfall that enters into the catchment is one of the main inputs which determine the runoff and erosion process in that watershed.
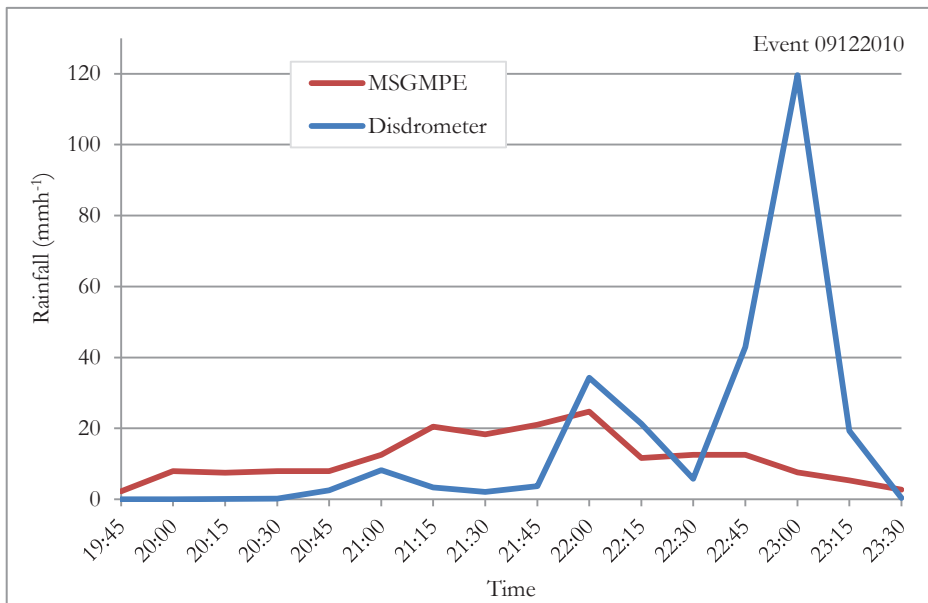
Figure 4-10: Hyetograph of rainfall (mmh^{-1}) and duration (time) comparison of the disdrometer and MSGMPE (intensity from MPE refers to the intensity of the pixel corresponding to disdrometer location) for the 09122010 event.

Table 4-10: Event characteristics (total rainfall, maximum intensity, total duration and EVI) measured by disdrometer and estimated by MSGMPE comparison of the 09122010 event.

Event Characteristics	09122010 Event	
	Disdrometer	MSGMPE
Total rainfall (mm)	66.0	46.0
Peak rainfall (mmh^{-1})	119.6	32.0
Total duration (min)	180	225
Event index (EVI)	43.83	6.54

For reasonable comparisons of the output simulated runoff and soil erosion results by modeling in the watershed from different sources of rainfall inputs, it is vital to make the total rainfall amounts the same from both sources that enter a watershed. Hence, since the total amount of the rainfall from disdrometer (66 mm) and MSGMPE (46 mm) were different for the selected event (Table 4-10), a ratio correction factor was adapted (see section 3.7). Therefore, the total amount of rainfall from both sources become the same (66 mm), after adapting MSGMPE rainfall to disdrometer measured rainfall(mm) and used as LISEM input for runoff and soil erosion modeling (Chapter 5).

5.   RUNOFF AND SOIL EROSION MODELING

5.1   Total rainfall over the catchment

To examine the spatial variation of infiltration, runoff and soil erosion in the study area, a simulation with homogeneous rainfall (derived from disdrometer) and spatially variable rainfall estimated by MSGMPE down scaled from 3 km to 20 m with nearest neighbourhood (NN) and inverse distance weighted (IDW) interpolations for the event 09122010 was studied.

Figure 5-1 shows the total amount of rainfall over the Ribeira Seca catchment that was estimated by MSGMPE and interpolated with nearest neighbor and inverse distance weight adapted to the disdrometer measurement by ratio factor for the 009122010 event. It is observed that unlike nearest neighbourhood, IDW interpolation depicts smoother results and provided better identification of a location where the highest (north western) rainfall occurred in the catchment. However, the NN interpolation depicts larger areas with high rainfall amounts (the whole north eastern and north western part) without identifying particular locations where the highest rainfall occurs in the catchment.
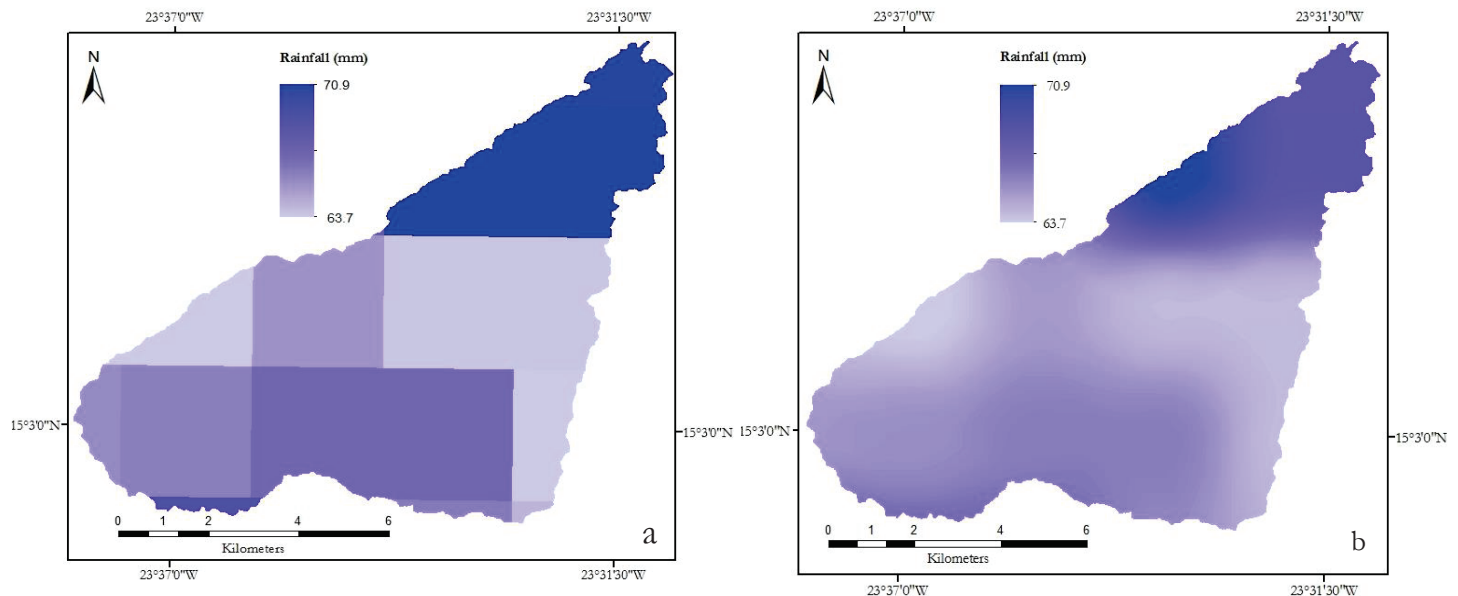
Figure 5-1: Total rainfall (mm) over Ribeira Seca catchment (estimated by MSGMPE) used as an input to LISEM for 09122010 event after correction: a) from nearest neighbourhood and b) from inverse distance weighted interpolations.

5.2   Infiltration simulation

Figure 5-2 presents the storage capacity (mm) calculated over the catchment and the cumulative infiltration pattern maps obtained from the disdrometer measured and satellite estimated (interpolated with the two methods) rainfall inputs. The storage capacity map is calculated from soil depth, porosity and initial moisture content of soil property maps used as input to LISEM model. The result reveals that there is a slight difference in cumulative infiltration pattern distribution over the Ribeira Seca catchment. The slightly higher in cumulative infiltration values of MSGMPE rainfall input over the entire catchment than that of the disdrometer, could be attributed to the higher intensity rain (hence exceeding the infiltration rate of the soil) measured by the disdrometer which produces runoff (Hortonian overland flow) immediately. However, in the case of MSGMPE, since the estimated intensity was lower (also low in EVI), cumulative infiltration was higher. Nevertheless, the patterns of the cumulative infiltration from the three rainfall inputs were quite similar. Furthermore, the infiltration patterns from both rainfall inputs follow the storage capacity (Figure 5-2a) of the soil calculated over the entire catchment.
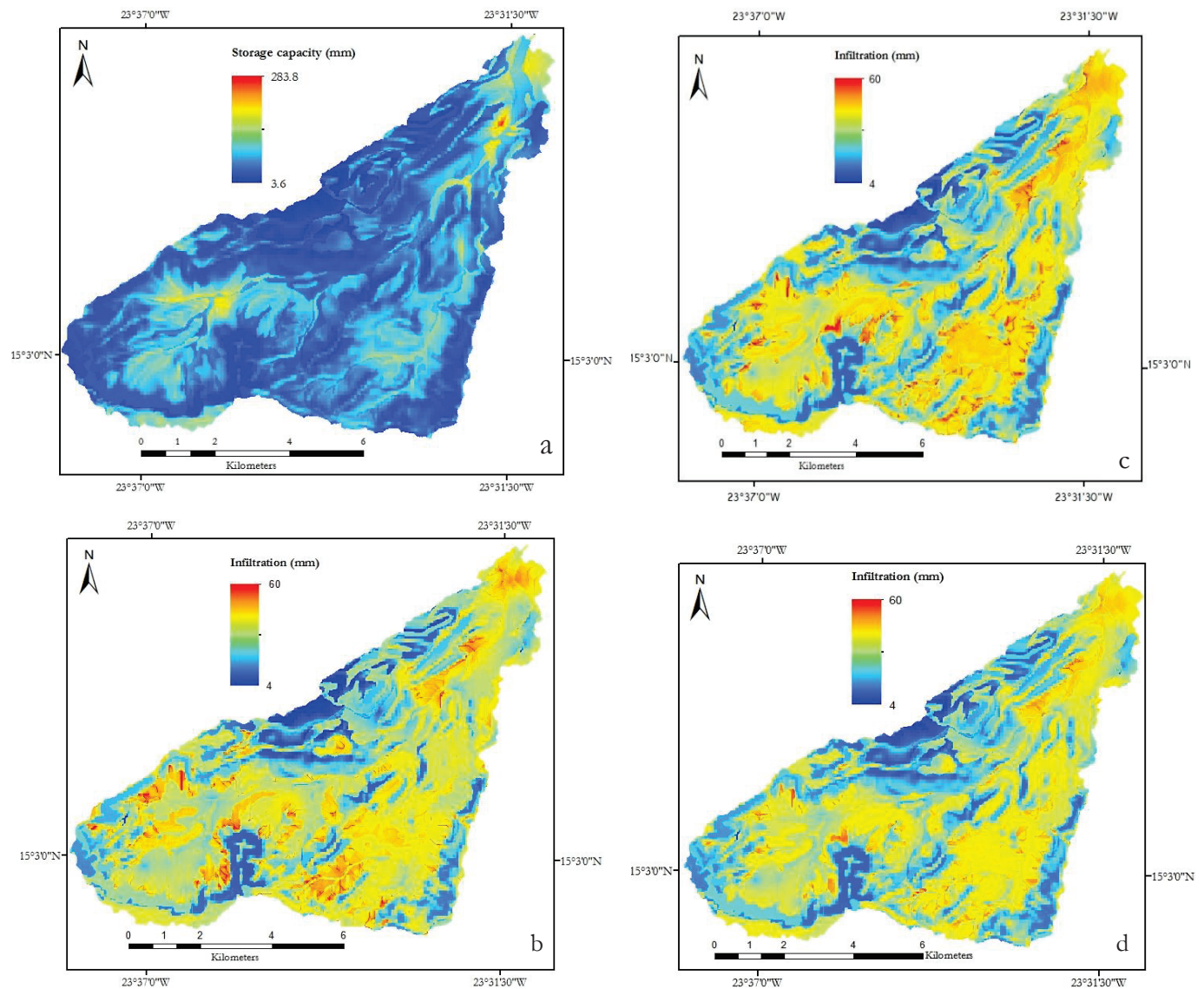
Figure 5-2: Storage capacity (a); and Spatial pattern of cumulative infiltrations over Ribeira Seca catchment for 09122010 event: b) with rainfall from disdrometer, b) with rainfall from MSGMPE interpolated by nearest neighbourhood, c) with rainfall from MSGMPE interpolated by inverse distance weighted.

It is found that the high values (Figure 5-3) of difference in cumulative infiltration follow the high storage capacity locations (Figure 5-2a) over the entire catchment. Furthermore, in almost all the location over the entire catchment the difference in infiltration values is > 0 mm, implying that there is a higher in cumulative infiltration with the rainfall from MPE input than with that of the disdrometer rainfall input. This could be attributed to either the lower intensity or the effect of the spatial variability of rainfall derived from MSGMPE. However, there are very limited places in which the cumulative infiltration from disdrometer rainfall input is higher than that of the MPE rainfall inputs.

Figure 5-3: The difference (subtraction of disdrometer infiltration from MSGMPE infiltration) in cumulative infiltration (mm) obtained.

Both cumulative infiltration simulation results depict in locations with very low porosity and cohesion (Figure 3-4), the infiltration was also very low for both rainfall inputs and vice versa. This can be evidenced by observing the north-west corner of the input porosity and cohesion maps where the porosity and cohesion are very low. It is apparent that the lower the porosity and cohesion, the lower is the infiltration rate, keeping the other parameters (for example, saturated hydraulic conductivity, land use, among others) constant.

5.3   Runoff simulation

Figure 5-4 shows the spatial pattern of runoff over Ribeira Seca catchment with homogeneous and spatially variable (with two methods of interpolation) rainfall inputs at time step of 360 minutes. This time step is a time just before the maximum runoff over the catchment is attained from MPE rainfall inputs. In both cases, the runoff commences at the north-west corner of the catchment (this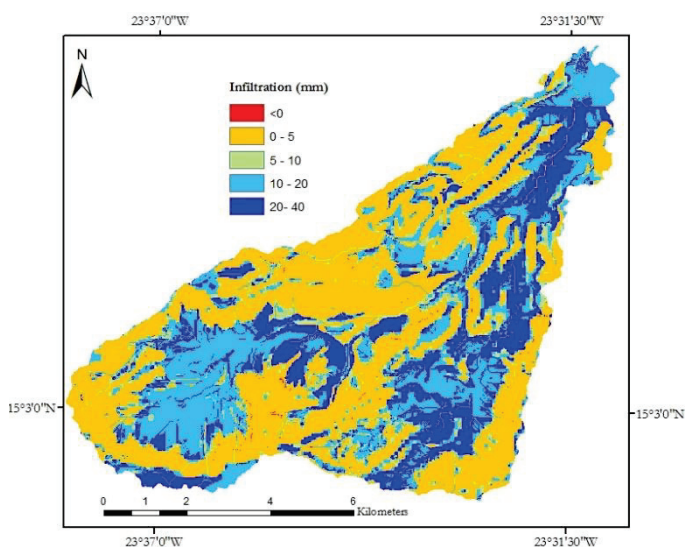 is the area with the lowest porosity and with low hydraulic conductivity) and gradually follows those areas with low porosity.

The spatial runoff pattern that resulted from disdrometer rainfall input was found to be higher at each run step and fills up the entire catchment at the time when the maximum runoff is attained. However, the one that from the MSGMPE derived rainfall inputs were low; spreads slowly over the catchment and did not fill the entire catchment at the maximum runoff time. But at 360 min the runoff pattern from MPE rainfall input shows higher values than disdrometer rainfall inputs at most parts of the north-east corner. These locations are also with high amount of rainfall is derived from MPE (Figure 5-1) and used in the input to the model. Therefore, this shows that the higher the rainfall amount the higher is the runoff generation. In this sense, it can be taken as an indication that MPE derived rainfall is able to simulate runoff for this event. In addition, satellite derived rainfall input gave better information in providing where the highest rainfall occurred in the catchment, hence with high runoff at that area as compared to the disdrometer measured rainfall input. Furthermore, this result gives an indication of the fact that both soil properties and amount of rainfall have an influence on the runoff generation in the catchment.
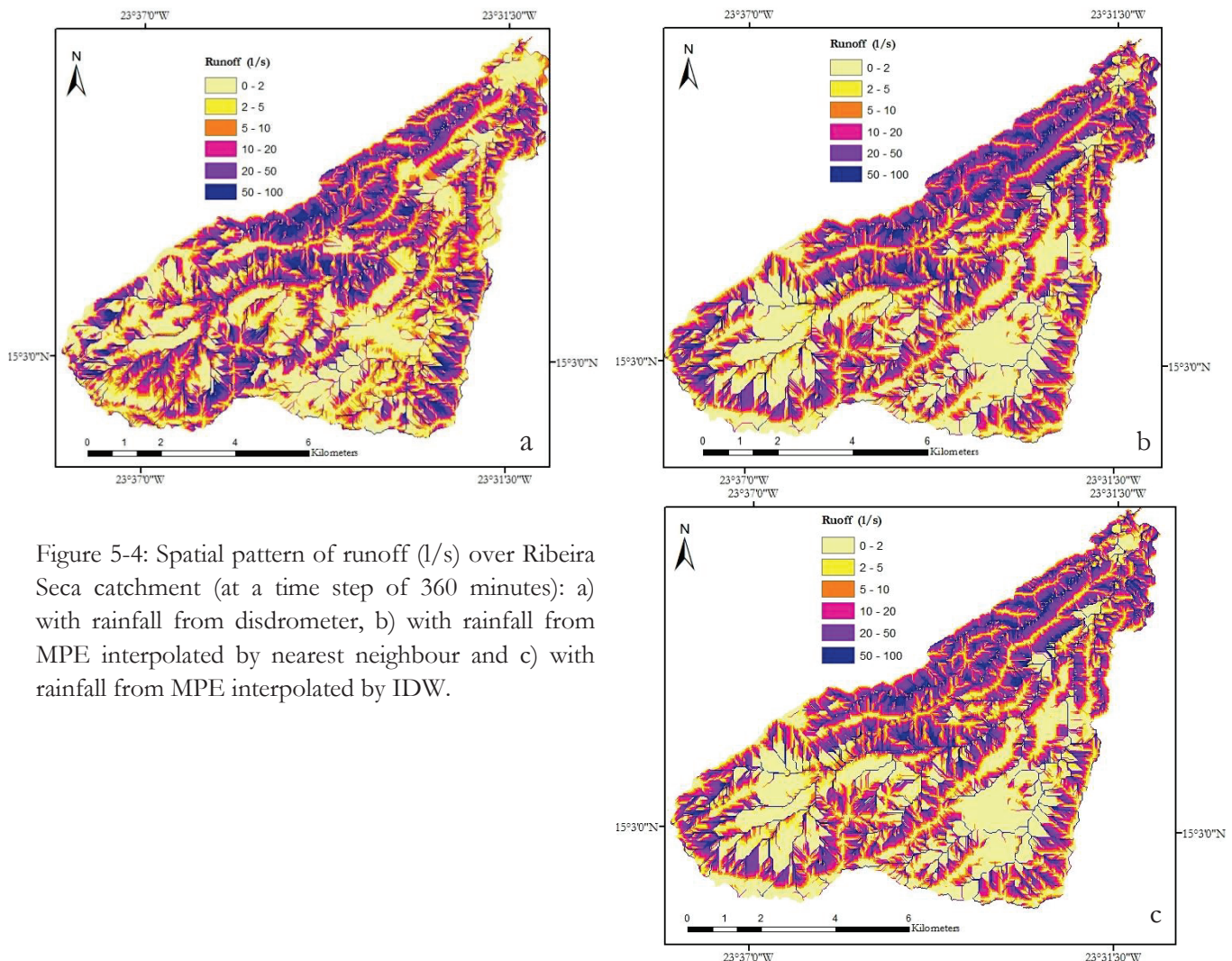
Figure 5-4: Spatial pattern of runoff (l/s) over Ribeira Seca catchment (at a time step of 360 minutes): a) with rainfall from disdrometer, b) with rainfall from MPE interpolated by nearest neighbour and c) with rainfall from MPE interpolated by IDW.

At the other remaining locations over the entire catchment, the runoff values from disdrometer measured rainfall input were higher for every runoff (l/s) class values. This can be evidenced, for example, by observing the center of south east part of the catchment. Moreover, at other time steps, for example at a time step (Figure 5-5) immediately before the maximum runoff is attained from disdrometer rainfall input, the runoff amount from disdrometer is higher. However there no significant difference in runoff pattern and values obtained from the two interpolation methods of satellite derived rainfall inputs. In general, the runoff patterns over the entire catchment from disdrometer and MSGMPE rainfall inputs are observed to be similar, and appear to follow the soil property used in the input maps (Figure 3-4).

Table 5-1 presents the summary of discharge and infiltration related results of the rainfall inputs that were measured by disdrometer and estimated by MSGMPE (with two methods of interpolations). It is observed that despite the total amount of rainfall over the catchment from disdrometer and MPE used as input to the model is the same, the results are different. For instance, the total discharge from disdrometer measured rainfall input higher than the MSGMPE rainfall inputs. The discharge to rainfall ratio in percentage also reveals higher (40.96%) in disdrometer than that from MSGMPE (25.58%) rainfall inputs. Furthermore, the total infiltration obtained confirms infiltration is higher in the MSGMPE rainfall input than that of the disdrometer measured rainfall input.

Even though the shapes of the hydrograph from the three rainfall inputs at the main outlet (Figure 5-6) were found to be similar and the total amount of rainfall that enters the catchment was the same, the total discharge, infiltration, the time of peak discharge and the amount of peak discharge were different (Table 5-1). The time occurrence of the peak discharge from disdrometer measured rainfall input was faster (at 347 min which is about less than double of the time (180.5 min) at which the peak rainfall occurred) than that from MSGMPE rainfall input (the peak discharge occurred at 333 min which is about triple of the time (120 min) occurrence of the peak rainfall). This could be attributed to the high intensity of disdrometer measured rainfall which translates immediately to runoff with Hortonian overland flow by exceeding the infiltration rate of the soil. On top of its high intensity, the rainfall from disdrometer lasts shorter duration (Table 4-10) than the rainfall from MSGMPE; therefore, has a better opportunity to contribute to more runoff amount. But in the case of MPE derived rainfall inputs, since the rainfall intensity was low and lasts longer duration, the runoff is generated after exceeding the storage capacity of the soil. This implies that most of the rainfall infiltrates, hence, lower in total discharge and other discharge related simulation results. Furthermore, the lower percentage of discharge to rainfall ratio from MPE rainfall inputs (25.58) than the disdrometer rainfall input (41.96) proves the aforementioned arguments. Nevertheless, the shape of the hydrograph and other discharge related simulations results from the two (NN and IDW interpolated) MSGMPE rainfall inputs were found to be the same show the same except slight difference (Table 5-1).

Table 5-1: Summary of discharge and infiltration related results from disdrometer measured and MSGMPE estimated (interpolated with two methods) rainfall inputs.

| Variables	Disdrometer	MSGMPE	
		NN Interpolation	IDW Interpolation
Time (min) of peak rainfall	180.5	120.5	120.5
Time (min) of peak discharge	347.0	332.5	333.0
Peak discharge (m³/s)	269.33	114.73	114.48
Total discharge (m³)	1,950.72	1,218.66	1,218.52
Total infiltration (mm)	36.48	46.63	46.65
Discharge/rainfall (%)	40.96	25.58	25.58

NN: Nearest Neighbourhood
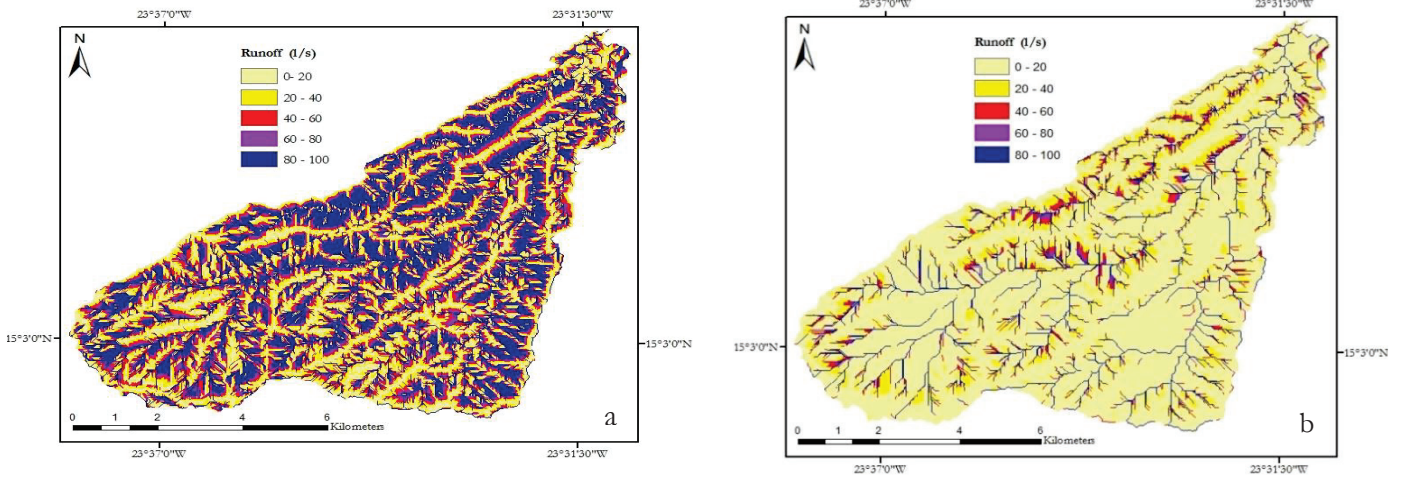
Figure 5-5: Spatial pattern of runoff (l/s) over Ribeira Seca catchment (at a time step of 368 minutes): a) with rainfall from disdrometer, b) with rainfall from MPE interpolated by nearest neighbourhood.

Figure 5-6: Shapes of the hydrograph at the main outlet of the catchment from disdrometer measured and MPE estimated (interpolated with two methods) rainfall inputs.

5.4   Soil erosion simulation
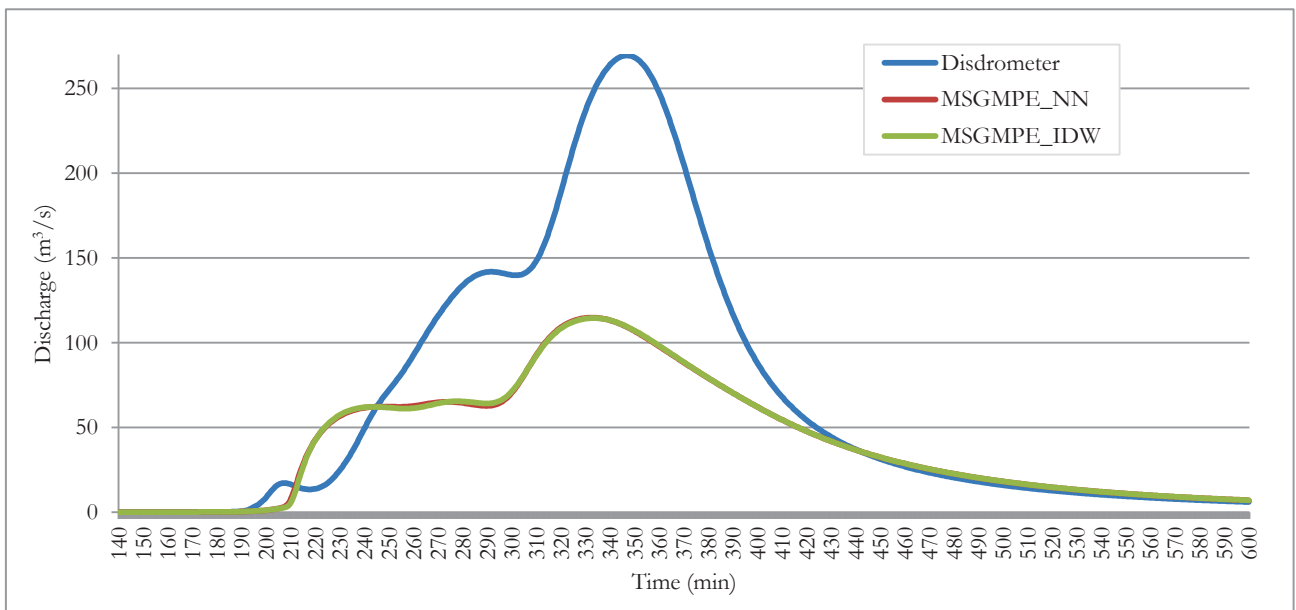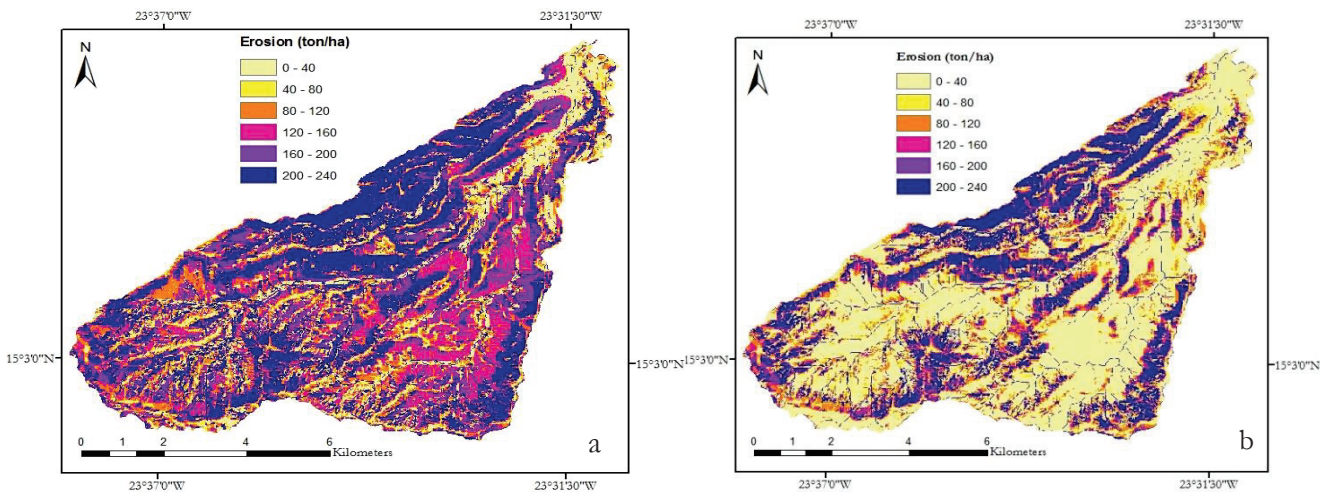

Figure 5-7: Spatial distribution of erosion (ton/ha) in Ribeira Seca catchment: a) with rainfall from disdrometer and b) with rainfall from MPE interpolated by nearest neighbourhood.

Figure 5-7 shows the distribution of erosion pattern in the catchment under the disdrometer measured and MSGMPE estimated (interpolated by NN) rainfall inputs. The erosion patterns show a similar pattern as runoff patterns. It is observed that, the locations affected mostly by erosion correspond to shallow soil depths (Figure 3-4c). In a similar was as runoff, areas affected by erosion in the catchment are more in the case of disdrometer rainfall input than the MSGMPE derived rainfall inputs.

Table 5-2 summarizes the total detachment, deposition, remaining suspended sediments and soil losses estimated by the three rainfall inputs. Despite the fact that the total amount of rain depth that enters the catchment from both measurements (disdrometer and MPE) the same, the simulated erosion and deposition related results are different. The splash detachment (land) from disdrometer rainfall input is $6.88 * 10^3$ ton; whereas, that from MSGMPE derived rainfall inputs are $6.45*10^3$ ton. The higher in the splash detachment from disdrometer rainfall input is attributed to the higher in intensity (rain drop), hence higher in the ability/energy of detaching the soil material. Similarly, the flow detachment (land), which is related to the amount of runoff, is higher for disdrometer measured rainfall input. Apparently this due to the reflection of higher in discharge obtained from disdrometer rainfall input which enables to detach the soil material by flowing water. The simulated sediment delivery ratio (the observed sediment yield at a location in the watershed to the total quantity of soil eroded in the catchment above that point) in percentage from MSGMPE derived rainfall input is about 3 times lower than that of the disdrometer measured rainfall input. This suggests that most of the detached sediments are deposited in the catchment before reaching the main outlet for the case of MSGMPE derived rainfall input than the disdrometer measured rainfall input. This is attributed to the low runoff, which allows deposition of the detached sediment along the way within the catchment rather than transporting to the outlet. This is further confirmed by the higher deposition of value (about $448 *10^3$ ton) of the sediment (land) obtained from the MSGMPE rainfall inputs. However, there is no such significant pattern and values difference resulted from the two (NN and IDW interpolated) MSGMPE rainfall inputs, except a very slight changes in values (Table 3-1).

Table 5-2: Total detachment, deposition, remaining suspended sediments (land and channels) and soil losses obtained from disdrometer and MSGMPE (interpolated with two methods) rainfall inputs for event 09122010.

Variables	Disdrometer	MSGMPE	
		NN Interpolation	IDW Interpolation
Land (*10³ ton)			
Splash detachment	6.88	6.45	6.44
Flow detachment	1,656.73	1,146.37	1,145.80
Deposition	345.25	447.8	447.4
Suspended sediment	6.08	4.83	4.84
Channels (*10³ ton)			
Flow detachment	171.74	280.84	280.69
Deposition	1,146	882.88	882.63
Suspended sediment	0.02	0.03	0.03
Soil loss			
Total soil loss (*10³ ton)	313.10	86.42	86.29
Average soil loss (ton/ha)	41.35	11.41	11.40
SDR (%)	17.06	6.03	6.02

NN: Nearest Neighbourhood

6.   CONCLUSIONS AND RECOMMENDATIONS

This chapter attempts to summarize the findings of the study, provide answers to the research questions formulated in Chapter 1 under sub-section 1.3.2 and finally foreward recommendations.

6.1   Summary and conclusions

How does satellite-derived rainfall correlate to the rain gauge and disdrometer measurements?

15 minutes temporal resolution based comparisons of the rain depth and intensity that is measured by disdrometer at a single location and estimated by MSGMPE showed poor (with a maximum of R^2 equals 0.34) correlations. Correlation between MSGMPE and ground measurements is improved as rainfall depths are aggregated to daily and compared per month and year than 15 minutes time. Daily based monthly comparison of rain depth estimated by MSGMPE with the rain depth measured by rain gauge and disdrometer reveals correlations with coefficient of determination (R^2) ranging from about 0.4 to 0.9 except for September 2009. Daily based yearly comparison of MSGMPE rainfall depth with measurements of rain gauge and disdrometer further reveals correlations with coefficient of determination (R^2) ranging from 0.3 to 05 and 0.3 to 0.6, respectively. 2010 is observed to be the year with the best correlation between MSGMPE and the ground based (rain gauge and disdrometer) rainfall measurements. In general, MSGMPE underestimated the rainfall (depth and intensity) that were recorded by disdrometer and rain gauge except a few days in which it overestimated the total rain depth.

The poor correlation obtained between MSGMPE and the ground based rainfall measurements, could be attributed to the fact that the rainfall from MSGMPE is based on cloud top temperature, hence indirect estimation of rainfall unlike rain gauge and disdrometer which record the actual rainfall on the ground. Therefore, the algorithm used to convert cloud top temperature to precipitation/rainfall and the structure of the atmospheric layer under the precipitating clouds determine the amount of the rainfall estimated by MSGMPE on the ground.

Which interpolation (down scaling 3 km MSGMPE to 20 m) method would give better simulation of runoff and soil erosion?

The results of the simulated infiltration, runoff and soil erosion spatial patterns obtained from the NN and IDW interpolated MSGMPE rainfall inputs showed no difference. Furthermore, the shapes of the hydrograph observed at the main outlet from both interpolation rainfall inputs are quite similar. Therefore, it can be concluded that there is no such significant difference in infiltration, runoff and soil erosion spatial patterns and amounts obtained from the NN and IDW interpolated MSGMPE rainfall inputs. However, the IDW interpolation method reveals a better result in identification of the location in the catchment where the highest rainfall occurs over the entire catchment. In addition, IDW interpolation showed a slightly lower in discharge and erosion values which could be due to the smooth rainfall surface over the entire catchment, unlike the NN interpolation method which shows blocky surfaces (therefore abrupt changes of rainfall value from one pixel to the other). Therefore, as to the conclusion, the IDW interpolation is better in showing the rainfall pattern over the entire catchment than the NN interpolation. This is because in reality, the rain doesn't change abruptly from one point to another within 3 km at least per 15 minutes time interval.

What are the temporal and spatial patterns of runoff and erosion processes within the watershed in homogeneous and spatially variable rainfall?

The results of the simulated infiltration, runoff and soil erosion spatial patterns obtained from the spatially variable MSGMPE rainfall inputs and that of the homogeneous rainfall measured by disdrometer input are observed to be similar in the selected event. In both rainfall inputs, the infiltration capacity of the soil in the catchment was reached in most of the locations at an early stage. However, the total infiltration, discharge and soil erosion obtained are quite different even though the total amount of rainfall (66 mm) that enters to the catchment is adapted to the same value.

Furthermore, despite the same amount of total rainfall that enters the catchment, the spatial patterns of runoff were different at different time steps. The lower values in total discharge and total soil erosion obtained from the satellite rainfall input could be related to either the lower in rainfall intensity (mmh^{-1}) or the spatial variability of rainfall. It is apparent that the high intensity from disdrometer measured rainfall (homogeneous) contributed to the higher results in total discharge (high runoff/low total infiltration), and high total erosion related results. In the MSGMPE rainfall inputs the location with the highest rainfall showed high runoff (low cumulative infiltration) and erosion. Other locations in the catchment (as for example north-west corner) show similar results, which are related to soil property (for example, storage capacity). Therefore, both the soil property and the rainfall amount determine the patterns and total amounts of runoff and soil erosion process in the catchment. As a summarized conclusion, the runoff patterns over the entire catchment from disdrometer and MSGMPE rainfall inputs are observed to be similar and appear to follow the soil property used in the input maps (Figure 3-4); whereas, the total results depict differences in values.

What is the difference in soil loss from the watershed in homogeneous rainfall and spatially variable rainfall?
Inspite of the fact that the total amount of rain depth that enters the catchment from both measurements (disdrometer and MSGMPE) the same, the simulated erosion and deposition related results are different. The splash detachment (land) from disdrometer rainfall input is 6.88 * 10^3 ton; whereas, that from MSGMPE derived rainfall inputs are 6.45*10^3 ton. In similar way as discussed above, the sediment delivery ratio (%) at the main outlet of the catchment obtained from the disdrometer rainfall (homogeneous) input is higher (17.1 %) than the MSGMPE rainfall inputs (6 %). This implies that in the case of the MSGMPE rainfall inputs, most of the detached sediments deposited in the catchment before reaching the main outlet. Other supportive justification for this conclusion is the discharge to rainfall ratio from disdrometer rainfall input is higher (41 %) as compared to that from the MSGMPE rainfall input (26 %). This indicates that about 41 % of the total rainfall from disdrometer input is translated to discharge; hence, able to carry more detached sediments to the main outlet.

6.2   Recommendations

- With the ratio factor corrected rainfall input, do calibration on 09122010 and on 08212010 events against the measured discharge available for these two events at control point 3 (Figure 3-2) and examine how realistic the calibration factors used.

- As it observed in this study, MSGMPE underestimated rainfall (intensity and rain depth), look for the other options how to correct the satellite data. One recommendation is download the MSG cloud temperature (IR channel 10.8 µm) images (Jeniffer et al., 2010) per 15 minute and apply Equation 3.1 (Sanchez Moreno et al., 2012b) to obtain modified intensity per 15 minute. Compare the results with the intensity from disdrometer measurement (see section 4.2) per 15 minutes and examine if correlation is improved. If the correlation is improved (to an acceptable level), use the equation of the improved correlation to correct the MSGMPE rainfall intensity to the disdrometer measured rainfall intensity.

- Finally, use the newly derived intensity (for the events with best correlation) to LISEM input and compare the results (infiltration, runoff, soil erosion, among many others) with the homogeneous rainfall input results for the respective event.

6.3   Limitations

- This research was done in Ribeira Seca catchment (71.5 km2), where only one disdrometer measurement of rainfall (mmh^{-1}) with high temporal resolution (3 minutes) is available. In reality a single point measurement could not represent such large area, which has a high difference in relief. Furthermore, this measurement data is available from only 1 of September 2008 to 16 of September 2010.
- Ideally, the ground based measurement of the rainfall that could be used for comparisons with the satellite estimate rainfall data, should be at other several different locations in the catchment, taking into account the altitude differences, leeward and windward directions.

LIST OF REFERENCES

Amato, U., Antomadis, A., Cuomo, V., Cutillo, L., Franzese, M., Murino, L., & Serio, C. (2008). Statistical cloud detection from SEVIRI multispectral images. [Article]. *Remote Sensing of Environment, 112*(3), 750-766. doi: 10.1016/j.rse.2007.06.004

Assouline, S., & Mualem, Y. (2006). Runoff from heterogeneous small bare catchments during soil surface sealing. [Article]. *Water Resources Research, 42*(12). doi: 10.1029/2005wr004592

Assouline, S., Selker, J. S., & Parlange, J. Y. (2007). A simple accurate method to predict time of ponding under variable intensity rainfall. [Article]. *Water Resources Research, 43*(3). doi: 10.1029/2006wr005138

Baartman, J. E. M., Jetten, V. G., Ritsema, C. J., & de Vente, J. (2012). Exploring effects of rainfall intensity and duration on soil erosion at the catchment scale using openLISEM: Prado catchment, SE Spain. *Hydrological Processes, 26*(7), 1034-1049. doi: 10.1002/hyp.8196

Broxton, P. D., Troch, P. A., & Lyon, S. W. (2009). On the role of aspect to quantify water transit times in small mountainous catchments. [Article]. *Water Resources Research, 45*. doi: 10.1029/2008wr007438

Capra, A., Mazzara, L. M., & Scicolone, B. (2005). Application of the EGEM model to predict ephemeral gully erosion in Sicily, Italy. *CATENA, 59*(2), 133-146. doi: 10.1016/j.catena.2004.07.001

Ceballos, A., Martínez-Fernández, J., & Luengo-Ugidos, M. Á. (2004). Analysis of rainfall trends and dry periods on a pluviometric gradient representative of Mediterranean climate in the Duero Basin, Spain. *Journal of Arid Environments, 58*(2), 215-233. doi: http://dx.doi.org/10.1016/j.jaridenv.2003.07.002

Chang, A. T. C., & Chiu, L. S. (1997). Uncertainty in satellite rainfall estimates: Time series comparison. *Advances in Space Research, 19*(3), 469-472. doi: http://dx.doi.org/10.1016/S0273-1177(97)00056-2

Chang, C. L. (2007). Influence of moving rainstorms on watershed responses. [Article]. *Environmental Engineering Science, 24*(10), 1353-1360. doi: 10.1089/ees.2006.0220

Cohen, M. J., Shepherd, K. D., & Walsh, M. G. (2005). Empirical reformulation of the universal soil loss equation for erosion risk assessment in a tropical watershed. *Geoderma, 124*(3–4), 235-252. doi: http://dx.doi.org/10.1016/j.geoderma.2004.05.003

Collischonn, B., Collischonn, W., & Tucci, C. E. M. (2008). Daily hydrological modeling in the Amazon basin using TRMM rainfall estimates. *Journal of Hydrology, 360*(1–4), 207-216. doi: 10.1016/j.jhydrol.2008.07.032

Coulthard, T. J., Macklin, M. G., & Kirkby, M. J. (2002). A cellular model of Holocene upland river basin and alluvial fan evolution. [Article]. *Earth Surface Processes and Landforms, 27*(3), 269-288. doi: 10.1002/esp.318

De Roo, A. P. J., & Jetten, V. G. (1999). Calibrating and validating the LISEM model for two data sets from the Netherlands and South Africa. *CATENA, 37*(3–4), 477-493. doi: 10.1016/s0341-8162(99)00034-x

De Roo, A. P. J., & Offermans, R. J. E. (1995). LISEM: a physically-based hydrological and soil erosion model for basin-scale water and sediment management. *Modelling and management of sustainable basin-scale water resource systems Proc. international symposium, Colorado, 1995, 231*, 399-407.

De Roo, A. P. J., Offermans, R. J. E., & Cremers, N. H. D. T. (1996b). LISEM: A single-event physically based hydrological and soil erosion model for drainage basins. II: sensitivity analysis, validation and application. *Hydrological Processes, 10*(8), 1119-1126. doi: 10.1002/(sici)1099-1085(199608)10:8<1119::aid-hyp416>3.0.co;2-v

De Roo, A. P. J., Wesseling, C. G., & Ritsema, C. J. (1996a). LISEM: A single-event physically based hydrological and soil erosion model for drainage basins. I: theory, input and output. *Hydrological Processes, 10*(8), 1107-1117. doi: 10.1002/(sici)1099-1085(199608)10:8<1107::aid-hyp415>3.0.co;2-4

de Vente, J., Poesen, J., Verstraeten, G., Van Rompaey, A., & Govers, G. (2008). Spatially distributed modelling of soil erosion and sediment yield at regional scales in Spain. *Global and Planetary Change, 60*(3–4), 393-415. doi: 10.1016/j.gloplacha.2007.05.002

DESIRE. (2012). DESIRE: Study site description. 04 Oct.2012: Retrived from :http://www.desire-his.eu/en/ribeira-seca-cape-verde/152-ribeira-seca-cape-verde-study-site-description.

Ebert, E. E., & Manton, M. J. (1998). Performance of satellite rainfall estimation algorithms during TOGA COARE. *Journal of the Atmospheric Sciences, 55*(9), 1537-1557.

ESSRI. Arc GIS Desktop 9.3 Help. Cell size and resamplig in analysis. 09 Sept 2012. Retrieved from:http://webhelp.esri.com/arcgisdesktop/9.3/index.cfm?TopicName=Cell%20size%20and%20resampling%20in%20analysis.

Evora Ferreira Querido, A. L. (1999). *Watershed system analysis for evaluating the efficiency of soil and water conservation works : a case study in Ribeira Seca, Santiago Island, Cape Verde.* ITC, Enschede.

Haile, A. T., Jetten, V. G., & Rientjes, T. H. M. (2010). *Rainfall variability and estimation for hydrologic modeling : a remote sensing based study at the source basin of the Upper Blue Nile river.* 166, University of Twente Faculty of Geo-Information and Earth Observation (ITC), Enschede. Retrieved from http://www.itc.nl/library/papers_2010/phd/haile.pdf

Haregeweyn, N., Poesen, J., Nyssen, J., De Wit, J., Haile, M., Govers, G., & Deckers, S. (2006). Reservoirs in Tigray (Northern Ethiopia): Characteristics and sediment deposition problems. [Article; Proceedings Paper]. *Land Degradation & Development, 17*(2), 211-230. doi: 10.1002/ldr.698

Heinemann, T. (2003). MPE validaion status report. Technical report. EUTMETSAT.

.

Hessel, R. (2005). Effects of grid cell size and time step length on simulation results of the Limburg soil erosion model (LISEM). *Hydrological Processes, 19*(15), 3037-3049. doi: 10.1002/hyp.5815

Hessel, R., Jetten, V., Liu, B., Zhang, Y., & Stolte, J. (2003b). Calibration of the LISEM model for a small Loess Plateau catchment. *CATENA, 54*(1–2), 235-254. doi: 10.1016/s0341-8162(03)00067-5

Hudson, N. (1986). *Soil conservation* (Second edition ed.). London: B.T. Batsford.

Jeniffer, K., Su, Z., Woldai, T., & Maathuis, B. (2010). Estimation of spatial–temporal rainfall distribution using remote sensing techniques: A case study of Makanya catchment, Tanzania. *International Journal of Applied Earth Observation and Geoinformation, 12, Supplement 1*(0), S90-S99. doi: 10.1016/j.jag.2009.10.003

Jetten, V. (2002). LISEM Limburg Soil Erosion Model User Manual. *Volume 2.x*, (Pp.64).Retrived from: http://www.itc.nl/lisem/download/lisemmanualv62x.pdf.

Jetten, V. (2011). Open LISEM. Welcome.26 September 2012. Retrived from :http://lisem.sourceforge.net/?page_id=62.

Jetten, V., de Roo, A., & Favis-Mortlock, D. (1999). Evaluation of field-scale and catchment-scale soil erosion models. *CATENA, 37*(3–4), 521-541. doi: 10.1016/s0341-8162(99)00037-5

Jetten, V., & Favis-Mortlock, D. (2006). Modelling Soil Erosion in Europe *Soil Erosion in Europe* (pp. 695-716): John Wiley & Sons, Ltd.

Jetten, V., Govers, G., & Hessel, R. (2003). Erosion models: Quality of spatial predictions. *Hydrological Processes, 17*(5), 887-900. doi: 10.1002/hyp.1168

Jetten, V., Poesen, J., Nachtergaele, J., & van de Vlag, D. E. (2006). Spatial modelling of ephemeral gully incision : a combined empirical and physical approach. *In: Soil erosion and sediment redistribution in river catchments : measurement, modelling and management / ed. by P.N. Owens and A.J. Collins. Wallingford : CABI International, 2006. ISBN 0-851-99050-9 pp. 209-220.*

Kidd, C., & Huffman, G. (2011). Global precipitation measurement. [Review]. *Meteorological Applications, 18*(3), 334-353. doi: 10.1002/met.284

Kunkel, K. E., Andsager, K., & Easterling, D. R. (1999). Long-term trends in extreme precipitation events over the conterminous United States and Canada. [Article]. *Journal of Climate, 12*(8), 2515-2527. doi: 10.1175/1520-0442(1999)012<2515:lttiep>2.0.co;2

Kværnø, S. H., & Stolte, J. (2012). Effects of soil physical data sources on discharge and soil loss simulated by the LISEM model. *CATENA, 97*(0), 137-149. doi: http://dx.doi.org/10.1016/j.catena.2012.05.001

Lal, R. (2001). Soil degradation by erosion. *Land Degradation & Development, 12*(6), 519-539. doi: 10.1002/ldr.472

Loffler-Mang, M., & Joss, J. (2000). An optical disdrometer for measuring size and velocity of hydrometeors. *Journal of Atmospheric and Oceanic Technology, 17*(2), 130-139.

Maathuis, B. H. P., Gieske, A. S. M., Retsios, V., van Leeuwen, B., Mannaerts, C. M., & Hendrikse, J. H. M. (2006). Meteosat - 8 : from temperature to rainfall. *In: ISPRS 2006 : ISPRS mid-term symposium 2006 remote sensing : from pixels to processes, 8-11 May 2006, Enschede, the Netherlands. Enschede : ITC, 2006. 5 p.*

Mannaerts, C. M., & Gabriels, D. (2000). Rainfall erosivity in Cape Verde. *Soil and Tillage Research, 55*(3–4), 207-212. doi: 10.1016/s0167-1987(00)00104-5

Martin-Vide, J., & Gomez, L. (1999). Regionalization of peninsular Spain based on the length of dry spells. *International Journal of Climatology, 19*(5), 537-555. doi: 10.1002/(sici)1097-0088(199904)19:5<537::aid-joc371>3.0.co;2-x

Mathugama, S., & Peiris, T. (2011). Critical Evaluation of Dry Spell Research: http://www.ijens.org/vol_11_i_06/114806-7575-ijbas-ijens.pdf.

Merritt, W. S., Letcher, R. A., & Jakeman, A. J. (2003). A review of erosion and sediment transport models. *Environmental Modelling & Software, 18*(8–9), 761-799. doi: 10.1016/s1364-8152(03)00078-1

Morgan, R. P. C. (2005). *Soil erosion and conservation* (Third edition ed.). Malden: Blackwell.

Morgan, R. P. C., & Davidson, D. A. (1986). *Soil erosion and conservation: Book*. New York: Longman Scientific & Technical.

Morgan, R. P. C., Quinton, J. N., Smith, R. E., Govers, G., Poesen, J. W. A., Auerswald, K., . . . Styczen, M. E. (1998). The European soil erosion model (EUROSEM): a dynamic approach for predicting sediment transport from fields and small catchments. *Earth Surface Processes and Landforms, 23*(6), 527-544. doi: 10.1002/(sici)1096-9837(199806)23:6<527::aid-esp868>3.0.co;2-5

Nyakatawa, E. Z., Reddy, K. C., & Lemunyon, J. L. (2001). Predicting soil erosion in conservation tillage cotton production systems using the revised universal soil loss equation (RUSLE). *Soil and Tillage Research, 57*(4), 213-224. doi: http://dx.doi.org/10.1016/S0167-1987(00)00178-1

Petan, S., Rusjan, S., Vidmar, A., & Mikoš, M. (2010). The rainfall kinetic energy–intensity relationship for rainfall erosivity estimation in the mediterranean part of Slovenia. *Journal of Hydrology, 391*(3–4), 314-321. doi: http://dx.doi.org/10.1016/j.jhydrol.2010.07.031

Pimentel, D., Harvey, C., Resosudarmo, P., Sinclair, K., Kurz, D., McNair, M., . . . Blair, R. (1995). Environmental and Economic Costs of Soil Erosion and Conservation Benefits. *Science, 267*(5201), 1117-1123. doi: 10.1126/science.267.5201.1117

Prasetia, R., As-syakur, A., & Osawa, T. (2012). Validation of TRMM Precipitation Radar satellite data over Indonesian region. *Theoretical and Applied Climatology*, 1-13. doi: 10.1007/s00704-012-0756-1

Prigent, C. (2010). Precipitation retrieval from space: An overview. *Comptes Rendus Geoscience, 342*(4–5), 380-389. doi: 10.1016/j.crte.2010.01.004

Ran, Q., Su, D., Li, P., & He, Z. (2012). Experimental study of the impact of rainfall characteristics on runoff generation and soil erosion. *Journal of Hydrology, 424–425*(0), 99-111. doi: 10.1016/j.jhydrol.2011.12.035

Renard, K. G., Foster, G. R., Weesies, G. A., McCool, D., & Yode, D. (1997). *Predicting soil erosion by water : a guide to conservation planning with the Revised Universal Soil Loss Equation RUSLE* (Vol. 703). Washington, D.C.: United States Department of Agriculture (USDA).

Salvador, P., Calle, A., Sanz, J., Rodriguez, J., & Casanova, J. L. (2013). An automatic self-learning cloud-filtering algorithm for Meteosat Second Generation-Spinning Enhanced Visible and Infrared Imager. [Article]. *Remote Sensing Letters, 4*(2), 180-189. doi: 10.1080/2150704x.2012.714086

Sanchez-Moreno, J. F., Mannaerts, C. M., Jetten, V., & Löffler-Mang, M. (2012a). Rainfall kinetic energy–intensity and rainfall momentum–intensity relationships for Cape Verde. *Journal of Hydrology, 454–455*(0), 131-140. doi: 10.1016/j.jhydrol.2012.06.007

Sánchez-Moreno, J. F., Mannaerts, C. M., & Jetten, V. G. (2008). Rainfall characterization by satellites and ground data for soil erosion estimation in Cape Verde. *In: ACRS 2008 : proceedings of the 29th Asian Conference on Remote Sensing, 10-14 November 2008, Colombo, Sri Lanka. Colombo : Survey Department of Sri Lanka, Asian Association on Remote sensing, 2008. 6 p.*

Sanchez Moreno, J. F., Jetten, V. G., & Mannaerts, C. M. (2012b). *power of rain : rainfall variability and erosion in Cape Verde.* 217, University of Twente Faculty of Geo-Information and Earth Observation (ITC), Enschede. Retrieved from http://www.itc.nl/library/papers_2012/phd/sanchez.pdf

Sandoval Gómez, M. R. (2007). *Spatial and temporal rainfall gauge data analysis and validation with TRMM microwave radiometer surface rainfall retrievals.* ITC, Enschede. Retrieved from http://www.itc.nl/library/papers_2007/msc/wrem/sandoval.pdf

Sheikh, V., van Loon, E., Hessel, R., & Jetten, V. (2010). Sensitivity of LISEM predicted catchment discharge to initial soil moisture content of soil profile. *Journal of Hydrology, 393*(3–4), 174-185. doi: 10.1016/j.jhydrol.2010.08.016

Stocking, M. A. (2003). Tropical Soils and Food Security: The Next 50 Years. *Science, 302*(5649), 1356-1359. doi: 10.1126/science.1088579

Tapiador, F. J., Turk, F. J., Petersen, W., Hou, A. Y., García-Ortega, E., Machado, L. A. T., . . . de Castro, M. (2012). Global precipitation measurement: Methods, datasets and applications. *Atmospheric Research, 104–105*(0), 70-97. doi: 10.1016/j.atmosres.2011.10.021

Thiemig, V., Rojas, R., Zambrano-Bigiarini, M., Levizzani, V., & De Roo, A. (2012). Validation of Satellite-Based Precipitation Products over Sparsely Gauged African River Basins. [Article]. *Journal of Hydrometeorology, 13*(6), 1760-1783. doi: 10.1175/jhm-d-12-032.1

Thies, B., & Bendix, J. (2011). Satellite based remote sensing of weather and climate: recent achievements and future perspectives. [Review]. *Meteorological Applications, 18*(3), 262-295. doi: 10.1002/met.288

Tolpekin, V. A., & Stein, A. (2012). *core of GIScience and earth observation : a process - based approach.* Enschede: University of Twente Faculty of Geo-Information and Earth Observation (ITC).

Ulbrich, C. W., & Miller, N. E. (2001). Experimental test of the effects of Z-R law variations on comparison of WSR-88D rainfall amounts with surface rain gauge and disdrometer data. [Article]. *Weather and Forecasting, 16*(3), 369-374. doi: 10.1175/1520-0434(2001)016<0369:etoteo>2.0.co;2

Verstraeten, G., & Poesen, J. (1999). The nature of small-scale flooding, muddy floods and retention pond sedimentation in central Belgium. [Article]. *Geomorphology, 29*(3-4), 275-292. doi: 10.1016/s0169-555x(99)00020-3

Viney, N. R., & Sivapalan, M. (1999). A conceptual model of sediment transport: application to the Avon River Basin in Western Australia. *Hydrological Processes, 13*(5), 727-743. doi: 10.1002/(sici)1099-1085(19990415)13:5<727::aid-hyp776>3.0.co;2-d

Wischmeier, W. H., & Smith, D. D. (1978). *Predicting rainfall erosion losses : a guide to conservation planning.* . Science and Education Administration United States Department of Agriculture (USDA) ; Purdue Agricultural Experiment Station.

Yuter, S. E., Kingsmill, D. E., Nance, L. B., & Loffler-Mang, M. (2006). Observations of precipitation size and fall speed characteristics within coexisting rain and wet snow. [Article]. *Journal of Applied Meteorology and Climatology, 45*(10), 1450-1464. doi: 10.1175/jam2406.1

APPENDICES

Appendix I: The detailed maps used as input to LISEM in the study.

Variable name	Map name	Method of map generation
Rainfall ID	id.map	derived from Disdrometer and MSGMPE
Catchment		
Catchment boundary	area.map	derived from DEM
Slope gradient (sine of slope in direction of flow)	grad.map	derived from DEM
Local surface Drainage Direction network	ldd.map	derived from DEM
Main catchment outlet	outlet.map	derived from DEM
Digital Elevation Model	dem.map	derived from 90m resolution SRTM
Land use		
Classified land use map	lu.map	derived from ALOS-ANVIR image of 2009
Leaf area index of the plant cover	lai.map	derived from per.map
Fraction surface cover by vegetation and residue	per.map	field observation from previous study
Plant height	ch.map	field observation from previous study
Surface maps		
Random roughness	rr_ked.map	derived from literature
Manning's n	n_lu.map	derived from literature
Width of impermeable roads	roadwidt.map	mapping from previous study
Fraction covered by stones (stoniness)	stonefrc.map	field observation from previous study
Fraction of grid cell covered by crust	crustfrc.map	field observation from previous study
Hard surface	hardsurf.map	derived from land cover map
Erosion		
Cohesion	cohes_ked.map	field observation
Extra cohesion factor by plant root	cohadd.map	derived from literature
Aggregate stability for splash erosion (aggregates)	cohes_ked.map	field observation from previous study
Median of texture of the suspended matter (D50)	d50.map	field observation from previous study
Infiltration related (Green and Amp 1st layer)		
Saturated hydraulic conductivity	ks_ked.map	field observation
Average suction at the wetting front	psi.map	derived from literature
Saturated soil moisture content (porosity)	poros_ked.map	field observation
Initial soil moisture content	moist_ked.map	field observation
Soil depth to bottom of layer 1	soildepth_ked.map	field observation
Channels		
Local drain direction of main channel network	lddchan.map	derived from LDD
Channel width	chanwidt.map	derived from LDD
Channel side angle	chanside.map	field observation
Channel gradient	changrad.map	derived from DEM
Manning's of channel bed	chanman.map	derived from literature
Cohesion of channel bed	chancoh.map	derived from literature
Infiltration rate of channel bed	chanksat.map	derived from literature

Appendix II: Scatter plot of daily rain depth yearly comparisons measured by rain gauge and disdrometer: a) 2008, b) 2009 and c) 2010 years.
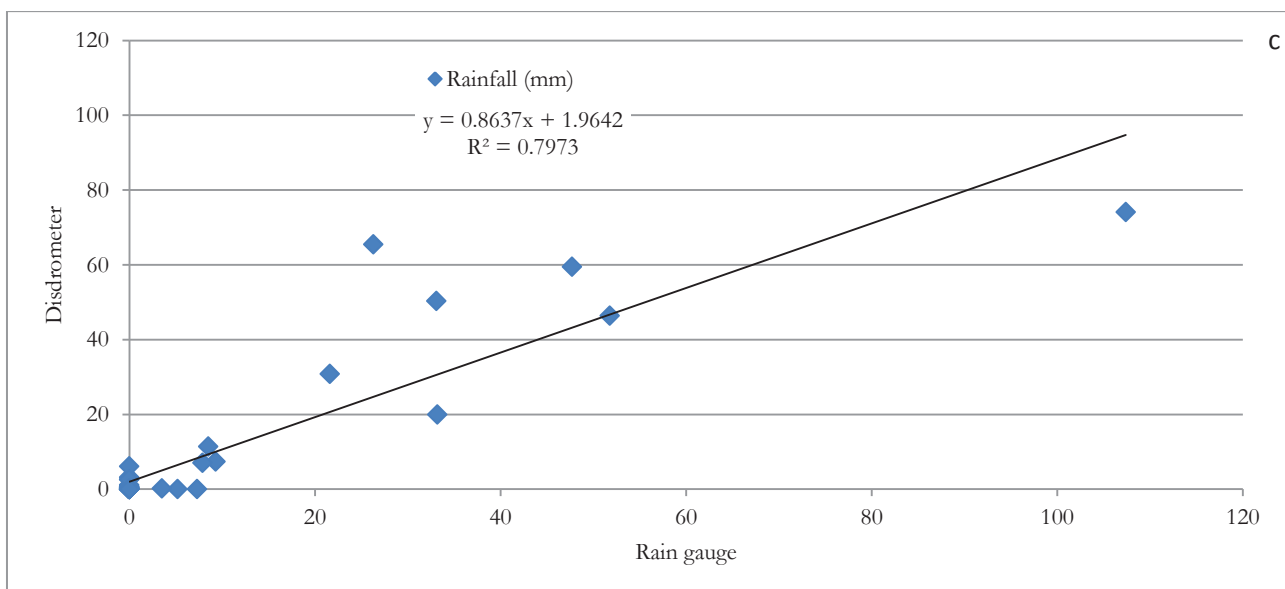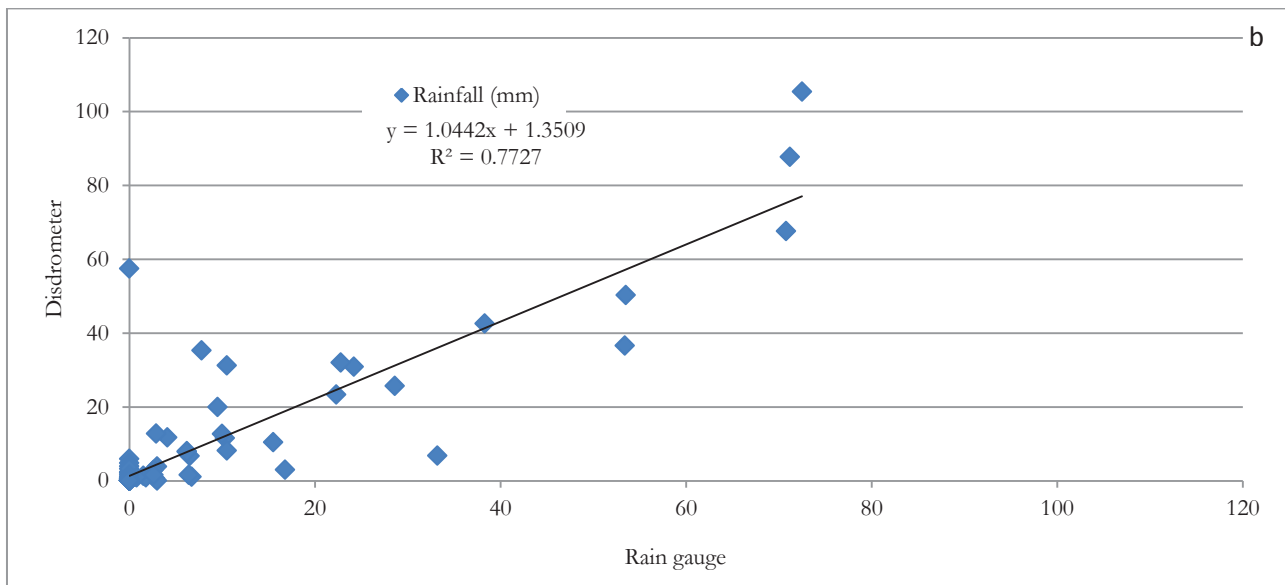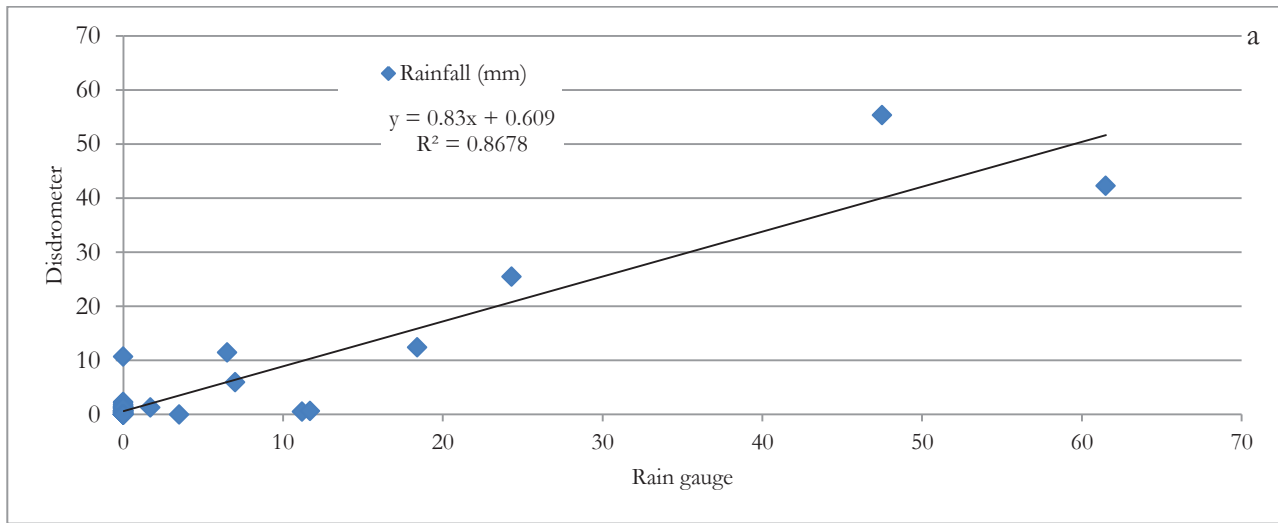
Appendix III: Scatter plot of daily rain depth yearly comparisons measured by rain gauge and estimated by MSGMPE a) 2008, b) 2009 and c) 2010 years.
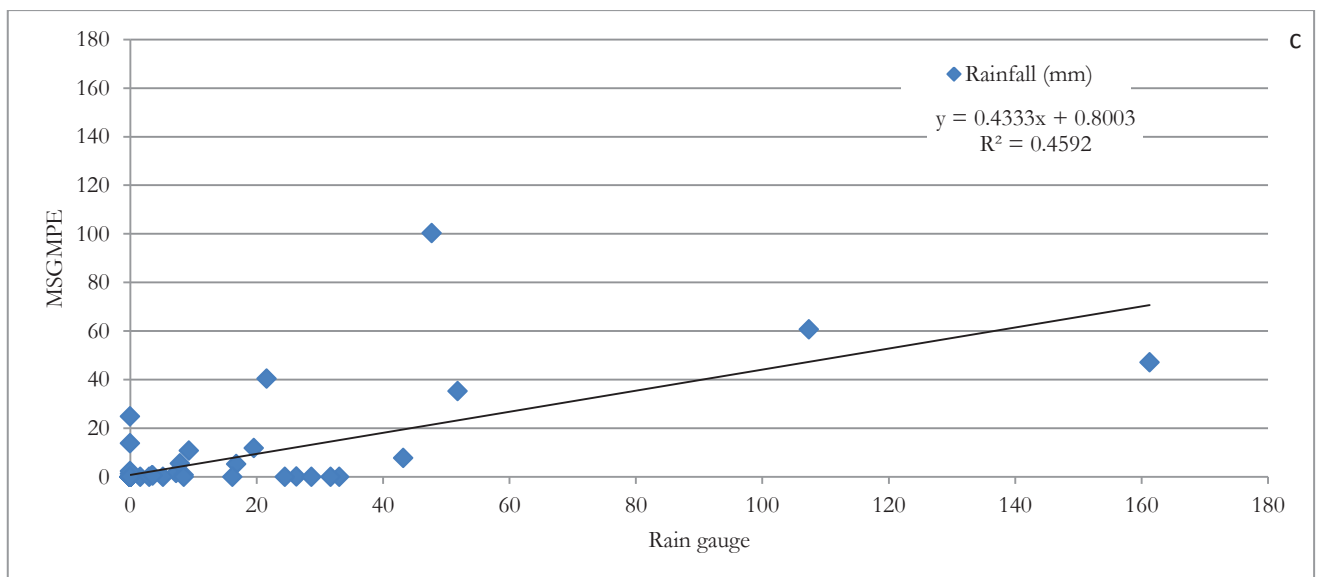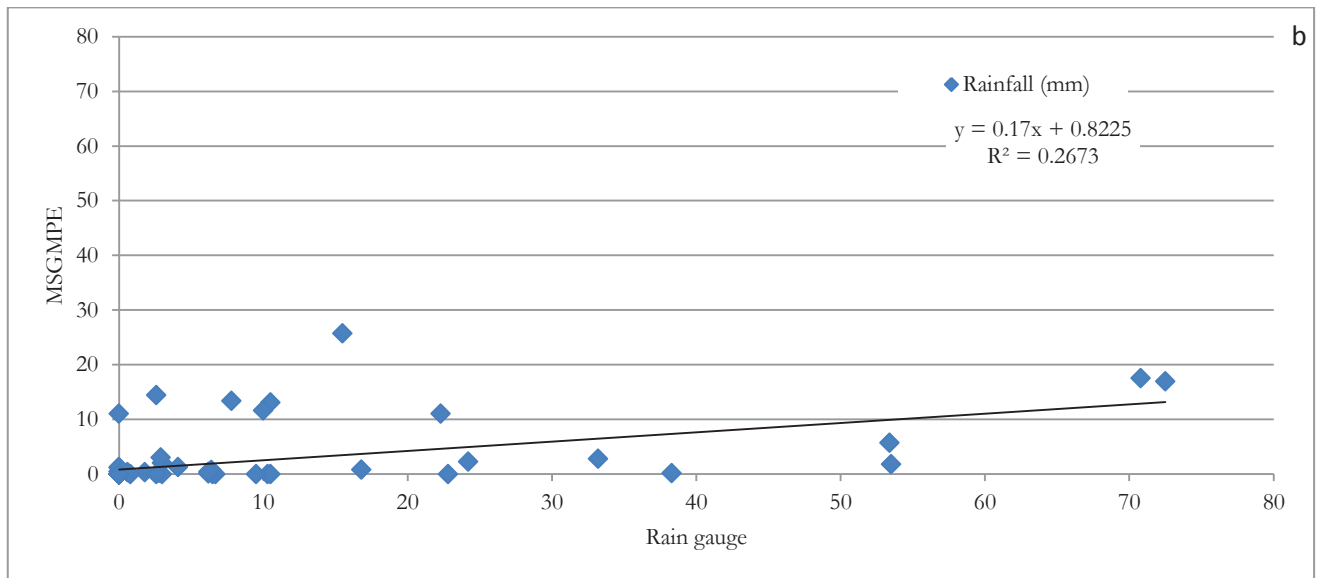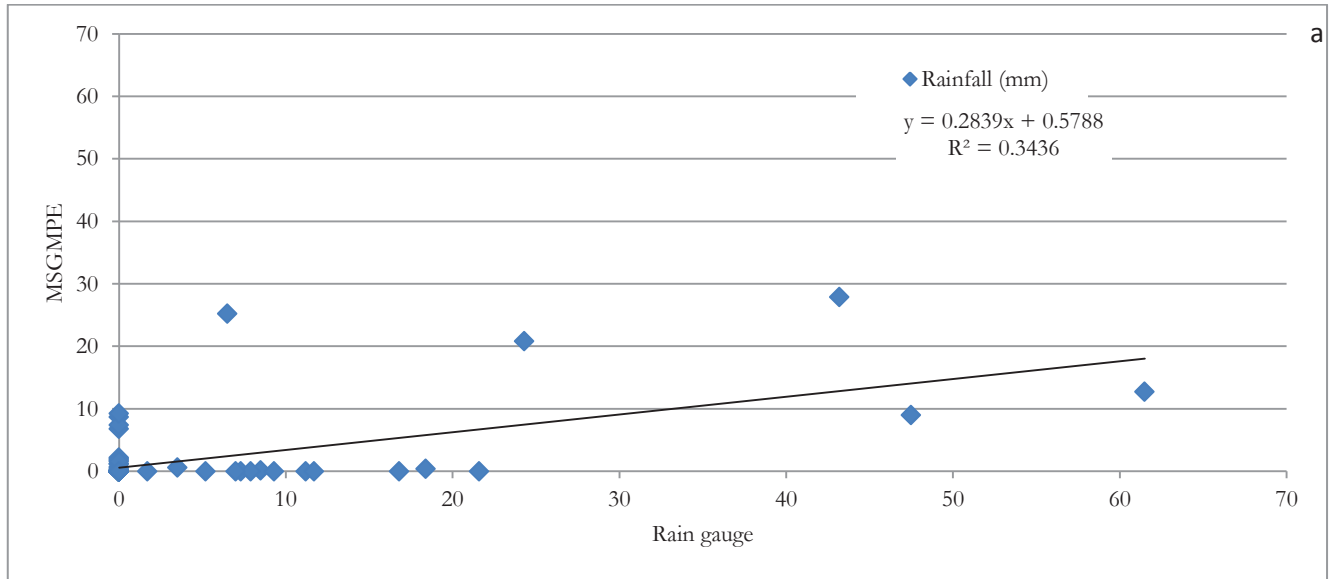
Appendix IV: Scatter plot of daily rain depth yearly comparisons measured by disdrometer and estimated by MSGMPE: a) 2008, b) 2009 and c) 2010 years.